Summer 8-25-2019

Zygote gene expression and plasmodial development in Didymium iridis

Sean Schaefer
DePaul University, seanschaefer@att.net

Zygote gene expression and plasmodial development in *Didymium iridis*

A Thesis presented in
Partial fulfillment of the
Requirements for the Degree of
Master of Biology

By
Sean Schaefer
2019

Advisor: Dr. Margaret Silliker

Department of Biological Sciences
College of Liberal Arts and Sciences
DePaul University
Chicago, IL

Abstract:

Didymium iridis is a cosmopolitan species of plasmodial slime mold consisting of two distinct life stages. Haploid amoebae and diploid plasmodia feed on microscopic organisms such as bacteria and fungi through phagocytosis. Sexually compatible haploid amoebae act as gametes which when fused embark on an irreversible developmental change resulting in a diploid zygote. The zygote can undergo closed mitosis resulting in a multinucleated plasmodium. Little is known about changes in gene expression during this developmental transition. Our principal goal in this study was to provide a comprehensive list of genes likely to be involved in plasmodial development. We performed suppressive subtractive hybridization to create cDNA libraries enriched for zygote or plasmodial specific genes. The cDNA libraries were then cloned and sequenced. The sequences were used to search against GenBank gene databases to identify related sequences and characterized proteins. We have compiled a list of candidate genes likely to be involved in the amoebae-zygote transition and have arranged them by their known or predicted function. Genes related to cytoskeletal structure, cell signaling, ubiquitin-proteasome pathways, mitochondrial inheritance, and DNA binding proteins were of particular interest due their possible role in this developmental transition. Selected gene sequences were also tested for differential expression by dot blot and RT-PCR.

Acknowledgements:

I would like to thank my advisor Dr. Margaret Silliker for her time and patience in helping me accomplish this project. Her expertise has helped tremendously in my writing, critical thinking and especially labwork and for that I am grateful.

I would like to thank my thesis committee Dr. William Gilliland and Dr. John Dean for their advice and assistance. I would like to thank my graduating cohort for their criticism and Sara Teemer for listening to my rants.

A special thanks to my lab partners Uri Baray for his help and companionship, and Taylor Harris for her help in the collection and analysis of sequence data. Lastly, I would like to thank Allison Meyer for her love and support which helped me through this process.

Table of Contents:

Results

Appendices

Introduction:

Didymium iridis belongs to the kingdom Amoebozoa in the phylum Mycetazoa. This phylum includes the plasmodial slime molds including its well-studied relative, *Physarum polycephalum* **(**Fiore-Donno et al. 2008). Plasmodial slime molds, or myxomycetes, are found in virtually every ecosystem in the world (Stephenson and Stemphen 2000). Myxomycetes are unified by their atypical life cycle which features a haploid amoebal cell stage, as well as a multinucleated diploid plasmodial stage. Both stages are free-living and found commonly in soil and leaf litter. Sexually compatible haploid amoebae, or genetically identical diploid plasmodia, can undergo cell fusion resulting in a multinucleated plasmodium (Collins 1976).

The purpose of this study was to identify genes that are expressed shortly after haploid amoebae fuse to form a diploid zygote. Zygotes quickly develop into multinucleated plasmodia and as a result have many plasmodia-specific genes activated during this timeframe. (Turnock et al. 1981, Sweeney et al. 1987, Bailey 1995, Walter et al. 2013.) During zygote formation a variety of cellular activities occur which include an extended cell cycle, reorganization of cytoskeletal components, and extensive cell growth (Bailey et al. 1992). Also within early zygote development uniparental mitochondrial inheritance occurs where the zygote actively degrades one parental mitochondrial type while retaining and propagating the other (Silliker and Collins 1988, Moriyama et al. 2005). The extreme differences in cell structure between amoebael and plasmodial stages must require many stage-specific genes that are differentially transcribed at each distinct stage of the life cycle.

D. iridis was chosen for this study due to its ease of culturing in laboratory settings, as well having access to heterothallic strains showing a high mating efficiency and a near equal contribution of mitochondrial inheritance within progeny (Silliker et al. 2002). Relatively few

studies have focused on zygote development in *D. iridis* or other myxomycetes. Previous studies done in *P. polycephalum* have identified plasmodial-specific genes (T'Jampens et al. 1999, Solnica-Krezel et al. 1995, Bailey et al. 1999, Murray et al. 1994, Pinchai et al. 2006, Walter et al. 2013); this experiment focused on generating an enriched cDNA library of genes expressed very early during zygote development compared to the *P. polycephalum* studies which generated cDNA libraries at a later timepoint in plasmodial development (Turnock et al. 1981, Uyeda and Kohama 1987, Bailey et al. 1987, Sweeney et al. 1987). Previous studies also used an apogamic mutant strain of *P. polycephalum* which undergoes cell fusion between genetically identical haploid amoebae to form a haploid plasmodia. This mutant is a laboratory phenomenon and while it contains many benefits, it does not represent the natural ecology of myxomycetes. Heterothallic mating of *D. iridis* wild type strains may be a better way to represent the natural developmental processes of these organisms.

In this study we identified a list of genes expressed early during zygote development. Using suppressive subtractive hybridization, we created cDNA libraries enriched for zygote and plasmodial specific genes which we then cloned, sequenced, and characterized. Questions posed by this study include: What kind of genes are expressed early within the amoebal-plasmodial transition? Can nucleases involved in mitochondrial inheritance in *D. iridis* be identified*?* Will genes involved in plasmodial development, a stage unique to the myxomycetes, be found only within this group or will they have homology to genes in the Amoebazoa or other organisms?

Review of Literature:

Organism of study: Didymium iridis

The class of myxomycetes are common in virtually every ecosystem as predators of microorganisms (Collins and Betterley 1982). They share characteristics of both fungi and animals and as a result have been classified under a separate phylum, Mycetozoa (Fiorre-Donno et al. 2008). Their animal-like phagocytic feeding patterns make them of ecological significance, as they feed on many bacterial and fungal species (Collins and Betterley, 1982). The most conspicuous life stage of these organisms is their multinucleate cell mass, or plasmodium. This is a feature unique to the myxomycetes. In this life stage, the organism's nuclei and organelles divide without cell partitioning. This has made myxomycetes a topic of interest to cell cycle and cancer researchers (Walker et. al 2017). A plasmodium is formed when two mating competent amoebae or swarm cells fuse together to form a zygote. Genetically identical zygotes or plasmodia can fuse with each other or individually enlarge to form a multinucleate mass (Collins 1976). Under certain conditions plasmodia will form spore-bearing fruiting bodies by meiosis which appear similar to that of fungi. The spores are spread primarily by wind dispersal and germinate into haploid amoebae or swarm cells (Frederick 1990). A schematic of the life cycle is pictured in figure 1. *D. iridis* belongs to the order Physarales which includes the model organism *Physarum polycephalum.* A great deal of research regarding myxomycetes has focused on *D. iridis* and *P. polycephalum* due to their relative ease of cultivation in laboratory settings (Collins and Betterley 1982, Walker et. al 2017).

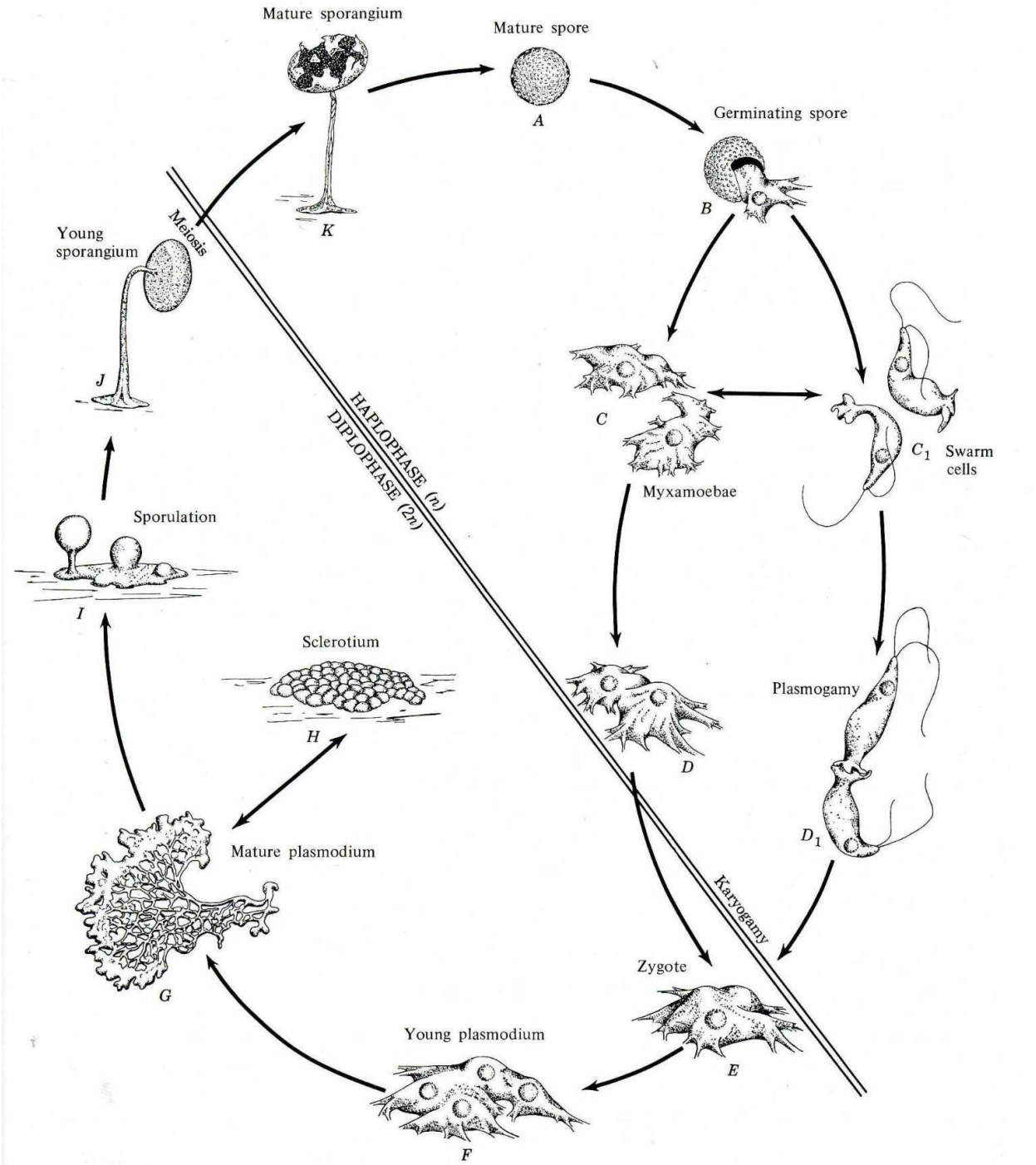

Figure 29-5 Life cycle of a typical heterothallic myxomycete. (A) Mature haploid spore. (B) Germinating spore. (C) Myxamoeba. Myxamoebae may encyst to form microcysts (not shown). (C_1) Swarm cells. (D) Fusing myxamoebae. (D_1) Fusing swarm cells. (E) Young zygote. (F) Young plasmodium. (G) Mature plasmodium. (H) Sclerotium. (I) Sporulation. (J) Young premeiotic sporangium with spores. (K) Mature postmeiotic sporangium. (Illustrated from living material by R. W. Scheetz.)

Figure 1. Life cycle: Introductory Mycology 1996 C.J. Alexopoulos, C. W. Mims, and M. Blackwell

Cell cycle and cytoskeletal rearrangement in P. polycephalum:

P. polycephalum is the most studied myxomycete in terms of plasmodial development; in particular with regards to the extended cell cycle and cytoskeletal rearrangement within zygotes. Much of this is due to the ability to culture apogomic (non-sexual fusion) and npf (non-plasmodia forming) mutants that are unavailable in other myxomycete species. *D. iridis* and *P. polycephalum* share a relatively close evolutionary relationship and many key characteristics such as: life cycle, plasmodial development, cytoskeletal rearrangement, and organelle inheritance patterns. Therefore, it is likely that homologous gene expression regulates these functions.

P. polycephalum features an extended cell cycle with a prolonged G2 phase upon haploid cell fusion; this results in extensive cell growth not seen in amoebal stages (Bailey et al. 1987, Bailey et al. 1992, Burland et al. 1993). A variety of genes and proteins (mostly cytoskeletal) have been shown to differ between the amoebal and plasmodial cell stages (Bailey 1995, Walter 2013). Zygotes grow to roughly twice the size of typical amoebae before proceeding to mitosis and as a result have a higher rate of protein synthesis than at any other point in the life cycle (T'Jampens et al. 1999). During this extended cell cycle, zygotes lose abilities unique to amoebal stages such as open mitosis and the ability to transform into a flagellated cell. An increase of tubulin production shortly before and during mitosis has been observed in *P. polycephalum* and is suggested to be involved in mitotic spindle formation (Laffler 1987). Zygotes gain abilities unique to plasmodia such as somatic fusion with other plasmodia and the ability to ingest myxomycete amoebae (Bailey et al. 1992). It has been estimated that as much as 5% of *P. polycephalum* genes are specific to either amoebae or plasmodia stages respectively (T'Jampens et al. 1999). This suggests a great deal of intracellular signaling and gene expression must take

place in a relatively short period of time to initiate the extensive cellular reorganization of both internal and external cell structure.

Perhaps the most significant changes in gene expression during plasmodial formation is in regard to the cytoskeleton composition and organization. Actin proteins are expressed at a high rate during the extended cell cycle and may provide the plasmodia with structural stability or specificity. Various actin-binding proteins such as profilin, tubulin, and fragmin have isotypes that are expressed in either amoebae or plasmodia. For example, in *P. polycephalum*, amoebae possess α3-tubulin isotype while plasmodia possess β2-tubulin isotype (Bailey 1995). It is unclear how the different tubulin isotypes change the function of the cytoskeleton, however it is interesting to note that three stage-specific cytoskeletal proteins have been identified and could represent one of many stage-specific proteins involved in cytoskeletal composition between haploid amoebae and diploid plasmodia.

Another actin binding molecule fragmin has different isotypes that are differentially expressed in amoebae and plasmodia; fragmin P is expressed in plasmodia and fragmin A in amoebae. Fragmin proteins function by binding actin molecules in the cytoskeleton creating an actin-fragmin kinase complex. Upon formation of this complex the kinase domain become activated furthering other downstream phosphorylation targets (T'Jampens et al. 1997, T'Jampens et al 1999). Due to fragmin's stage specificity and kinase activity it is a good candidate to be involved in plasmodial development and possibly cytoskeletal reorganization.

Other cytoskeletal proteins such as myosin have also been involved in cytoskeletal reorganization and plasmodial development. Myosin proteins are expressed continually throughout the life cycle of myxomycetes (Murray et al. 1994). It is unknown if stage-specific myosin isotypes exist in *D. iridis* but can be inferred due to the reliance of many plasmodial

specific traits on myosin proteins. For example, myosin proteins have been identified to be involved in cytoplasmic streaming (movement of fluid within the cell) as well as locomotion in the plasmodia (Murray et al. 1994). Both processes are unique to the plasmodia cell stage and would likely be initiated early during zygote development.

Mitochondrial inheritance mechanisms:

In eukaryotes there is a trend toward uniparental inheritance, where one parental mitochondrial DNA persists while the other is lost (Sato and Sato 2013). This phenomenon is evolutionarily favored across taxa due to an increased metabolic efficiency (Gray et al. 1999) and a reduction of incompatibility between nuclear and mitochondrial genomes (Eberhard 1980). This is accomplished by many different mechanisms (Breton and Stewart 2015). Gamete formation occurs in some animals and plants where mitochondria of the sperm or pollen is actively destroyed by ubiquitin proteins prior to zygote formation (Sato and Sato 2013, Yu et al. 2017). Autophagy of mtDNA post fertilization is a method utilized by *Caenorhabditis elegans,* among others (Sato and Sato 2013). Fish such as *Oryzias latipes* engage in mtDNA degradation both pre and post fertilization (Sato and Sato 2013). Other mechanisms, as seen in many fungal species, include dilution methods where one parent's mtDNA type is virtually nonexistent by selective replication of the other mtDNA (Barr et al. 2005). Biparental inheritance can also occur, although it is uncommon. Some species of fungi exhibit this with little to no adverse implications (Barr et al. 2005). In fact, it is speculated that low rates of biparental inheritance can clear out deleterious mutations within an organism's genome by recombination and can therefore benefit genetic integrity of the population (Hadjivasiliou et al. 2013).

Mitochondrial inheritance mechanisms in D. iridis and P. polycephalum:

Mitochondrial inheritance within myxomycetes has been an area of research for decades. Due to their unique life cycle they possess a novel and somewhat enigmatic mechanism for controlling mitochondrial inheritance. *P. polycephalum* and *D. iridis* are the most commonly studied myxomycetes with regard to mitochondrial inheritance and although their patterns of inheritance tend to vary somewhat, the molecular mechanisms for accomplishing uniparental inheritance appear to be very similar. The mechanism involves selective degradation (Kawano et al. 1987); the destruction of mtDNA from one parental cell with retention of the other and is achieved within 5 hours of zygote formation (Moriyama et al. 2005, Moriyama et al. 2009). DAPI staining of mitochondrial DNA revealed almost identical results when carried out with both *P. polycephalum* and *D. iridis* suggesting a conserved mechanism. The driving force behind selective degradation is carried out by nucleases. Evidence of nucleases have been uncovered in *P. polycephalum* (Moriyama et al. 2005) and can be inferred to be present in *D. iridis* as well (Silliker and Collins 1988, Silliker et al. 2002).

P. polycephalum has a definitive hierarchy in which a dominant mating type allele determines the mtDNA type that is retained within zygotes (Moriyama et al. 2003). This is determined by the *matA* allele located within the organism's nuclear genome. There are 14 *matA* alleles discovered so far, each with a predictable hierarchical inheritance pattern when mated with another compatible amoebae or swarm cell (Moriyama et al. 2003). *D. iridis* on the other hand does not show evidence of a hierarchical mitochondrial DNA donor system. However, *D. iridis* and *P. polycephalum* almost exclusively show uniparental mitochondrial inheritance (Moriyama et al. 2010, Silliker et. al 2002).

Myxomycetes have three factors that make them much different from other eukaryotes in terms of accomplishing uniparental inheritance of the mitochondria. First, they are isogamous, meaning the gametes are of the same size (Silliker and Collins 1988). Most animals utilize gamete size disparity to determine which will be the mitochondrial donor such as a large egg and small sperm cells. Second, myxomycete gametes fuse completely and proceed to closed mitosis without any subsequent cell division while other isogamous organisms, like yeast, divide repeatedly (Barr et al. 2005). This means that although there is initially biparental inheritance within myxomycetes, one parental mtDNA must be actively degraded within a relatively short time period to achieve uniparental inheritance. In comparison, yeast essentially dilute out one mtDNA population by cell division and mitochondrial segregation to achieve uniparental inheritance (Barr et al. 2005). Third, myxomycetes contain a multiple-sex mating system and cannot rely on a binary mating system to determine which cell will be the mitochondrial donor. The elements of isogamous fusion, lack of cell partitioning, and multiple mating types result in a novel mechanism of mitochondrial inheritance which has been proposed to be carried out by nucleases employed by the donor gamete.

Ubiquitin-proteasome system:

The ubiquitin-proteasome system is a highly conserved pathway amongst eukaryotes and is the primary system for protein catabolism. Ubiquitin serves as a molecular tag which is recognized by proteasome complexes, it is used as a marker to initiate the degradation of misfolded and unneeded proteins within the cell by proteasome complexes and autophagic organelles. The ubiquitin-proteasome system serves as the principal method for cellular proteostasis, or homeostasis of protein molecules (Zientara-rytter and Subramani 2019).

Ubiquitin molecules are 76 amino acids in length and are ligated onto proteins in both monomers and polymers (Nandi et al. 2006). The frequency at which ubiquitin molecules are ligated onto a protein is thought to determine the protein's fate. For example, mono-ubiquitin tags can initiate endocytosis and histone modification whereas polyubiquitination often results in the recruitment of degradative protein complexes and autophagy (Nandi et al. 2006). By nature, this system works in close tandem with organelles such as autophagic lysosomes, vacuoles and endoplasmic reticulum (Zientara-rytter and Subramani 2019). Despite the high conservation of the ubiquitin ligases across taxa (in particular E1 and E2 ligases), the diversity of proteasome complexes and the expression levels of these complexes can vary dramatically between organisms and cell types (Morozov and Karpov 2018). Different cells can harbor different populations of proteasome molecules which vary in substrate preference. Proteasome populations within a cell are fluid and can change by environmental and genetic factors (Morozov and Karpov 2018). For instance, mice use modified ubiquitin-proteasome proteins shortly after fertilization to recognize and degrade paternal mitochondrial DNA in the zygote (Sato and Sato 2013)**;** while other uses of the ubiquitin-proteasome system can include cellular communication, as some proteasomes secrete products into extracellular vesicles (Morozov and Karpov 2018).

An expanding hypothesis supports the concept that in addition to cellular proteostasis, the ubiquitin-proteasome system can have implications on other processes such as protein modification, cellular signaling and gene expression through the activation of transcription factors (Nandi et al. 2006). There are an estimated 5×10^{15} different proteasome substrate preferences (Morozov and Karpov 2018) implying that the specificity of ubiquitin-proteasome proteins is extremely high, particularly within E3 ligases (Nandi et al. 2006). There have been

hundreds of genes identified which encode E3 ligases in comparison to tens of genes encoding E2 ligases and only a few genes encoding E1 ligases (Nandi et al. 2006). This suggests that E3 and E2 ligases are needed to provide specificity of substrates while E1 ligases may have more general substrate preference. In addition to the diversity of substrate preferences, there exists many molecules which can alter the regulation and function of the ubiquitin-proteasome complex such as inhibitors and activators which can bind to proteasome complexes and alter both substrate preference and catalytic activity (Morozov and Karpov 2018). The role ubiquitin proteasome proteins play during plasmodial development is currently unknown but it could have an augmented function in general proteostasis.

Signal transduction in myxomycetes:

Considerable cell signaling research involving myxomycetes has been related to *P. polycephalum's* ability to sporulate in response to light flashes and its ability to propagate toward food sources and/ or chemoattractants (de Lacy Costello and Adamatzky 2014). At the cellular level, many studies have been dedicated to plasmodia's ability to synchronize nuclear events such as cell cycle arrest and cellular movements by intracellular transport known as cytoplasmic streaming (Walker et al. 2017). As a result, much of the published work on myxomycetes signal transduction involves the plasmodia's ability to respond to external stimuli and its capability to transport signals within a multinucleated cell (Alim et al. 2017, Walker et al. 2017). A recent study using *P. polycephalum* as a model organism analyzes the learning capabilities within unicellular plasmodia; long term habituation and recognition of deterrents are believed to be a result of extensive signal transduction (Bousard et al. 2018). Sporulation transcriptomics reveal extensive remodeling of signaling pathways during the plasmodia-sporangium transition

suggesting distinct signaling pathways are present within each stage of the life cycle (Barrantes et al. 2012, Glöckner and Marwan 2017). A relatively limited amount of information has been uncovered in terms of signal transduction as it relates to developmental pathways such as the amoebae-plasmodial transition.

Despite the lack of specific knowledge concerning myxomycetes signal transduction, these organisms appear to use many of the same pathways as other protists. G-proteins act as membrane receptors which initiate transcriptional and enzymatic modifiers through the use of signaling molecules such as cyclic NMP's (Heidel et al. 2011). One of the differentiating factors between signal transduction in the myxomycetes and others in the amoebozoa kingdom is their use of extensive cellular communication to synchronize nuclear division in a multinucleated plasmodia. Myxomycetes contain a higher number of genes that encode signaling proteins than their amoebal ancestors (Schaap et al. 2015). This can likely be attributed to their augmented life cycle compared to free living soil amoebae which don't have amoebal-plasmodial developmental pathways. The increase in signaling proteins may also be attributed to the plasmodia's necesity to initiate environmental responses within its multinucleated cell (Schaap et al. 2015).

Recent metagenomic analyses of the *P. polycephalum* genome have revealed new insights into signal transduction for myxomycetes. Such insights are especially useful when comparing the myxomycete signaling system to evolutionarily related taxa. Schaap et al. 2015 discovered many interesting findings related to myxomycete signaling by comparing genomic analyses of *P. polycephalum* to the cellular slime mold *Dictyostelium discoideum* and the amoebae *Acanthamoebae castellani*. Some of the major findings of this research were that *P. polycephalum* has a higher number of signaling molecules compared to the other two groups. These include a higher diversity of G-proteins, kinases, and cyclic nucleotide signals. There also

appears to be a significant amount of diversity within the alpha subunits of *P. polycephalum* G-proteins compared to the two other taxa, which can also be associated with the unique life cycle of myxomycetes and is perhaps an integral part of plasmodial development. More information is needed on specific G-protein functions within the myxomycetes to conclusively decode their individual protein functions. Similarly, G-proteins in the cellular slime molds tend to be more divergent while downstream targets and signaling molecules tend to be more conserved suggesting that G-proteins may provide novelty within species in the Mycetazoa phylum (Heidel et al. 2011). *P. polyecephalum* also displays roughly five times the amount of sensor histidine kinases/ phosphatases than *A. castellani* and *D. discoideum;* it is believed that the increase in these proteins are related to enzymatic or transcriptional activity and could play a significant role in plasmodial development (Schaap et al. 2015). Signal transduction within myxomycetes remains somewhat enigmatic and requires more biochemical testing in order to properly determine the roles different proteins play in plasmodial development and gene transcription; however, the presence of extensive signaling genes could be responsible for the alternate developmental pathways that are not seen in other related taxa.

Suppressive subtractive hybridization:

Subtractive hybridization combined with PCR can selectively amplify gene fragments unique to a cell type. This is referred to as suppressive subtractive hybridization, or SSH. In this method mRNA is extracted from two related cell types and converted to cDNA. The cDNA is first digested using *Rsa* I restriction enzyme to limit fragment size and to create blunt ends. One population of cDNA gets two different adapter sequences ligated onto the ends of the cDNA fragments and is referred to as the tester while the alternate cDNA population without adapters is

referred to as the driver. Mixtures of tester cDNAs are allowed to hybridize with unligated driver which have roughly 5 times the frequency of representation compared to tester. Shared fragments between the two cDNA libraries hybridize with each other while gene fragments unique to the tester populations get exponentially amplified using primers specific to the two adapter sequences. This results in a subtracted cDNA library containing gene products unique to one cell type (Diatchenko et al. 1996). An illustration of this mechanism can be seen in figure 2.

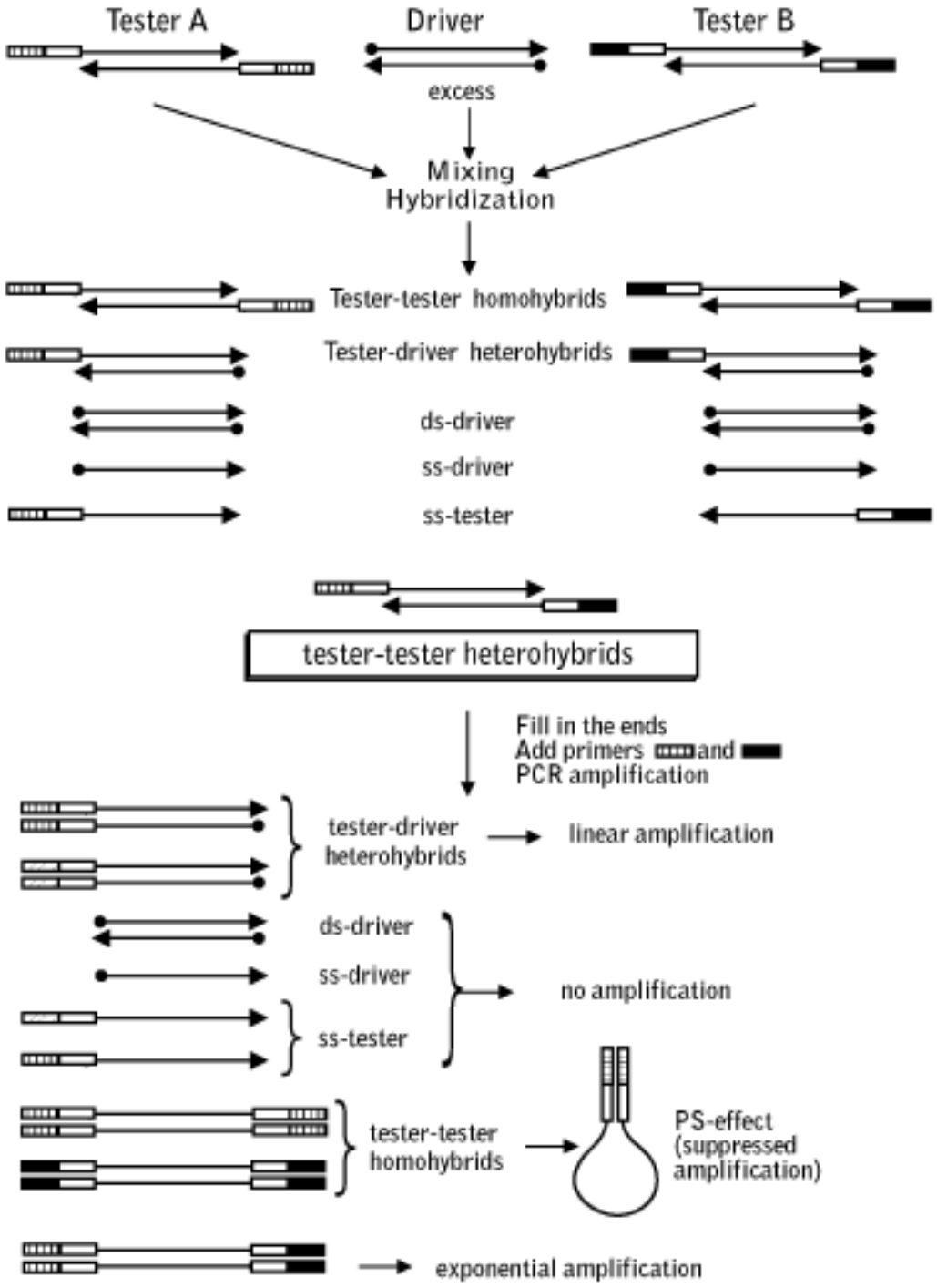

Figure 2. SSH schematic: taken from evrogen.com/technologies/SSH

Methods:

Strains and cultivation - The strains selected for this study were laboratory cultures belonging to the A1 Central American mating series (Clark et al 1991). These isolates were provided by Dr. Jim Clark who obtained them from the Collins mating type testers collection (Collins and Betterley 1982). Both Pan 2-44 (mating type A^7) and Hon 1-7 (mating type A^1) were selected due to their high mating efficiency (Silliker et al. 2002). Haploid amoebae were maintained in liquid axenic culture, peptone-glucose-yeast (PGY) and supplemented with heat killed bacteria (HKB) described in (Silliker et al. 1988). Both zygotes and plasmodia were formed by combining equal amounts of liquid haploid cultures onto half strength corn meal agar (CMA/2) solidified in cell culture flasks.

Determination of mating/collection time point – One challenge of this study was obtaining zygote mRNA which could then be subtracted from the amoebae and plasmodia cell stages. Due to the extreme similarities between zygotes and amoebae in size and overlap in development it is virtually impossible to gather mRNA from a culture containing only zygotes. Instead a mixture zygotes and amoebae were harvested at a time point in which the highest number of uninucleated zygotes were observed. Pilot studies consisting of frequent cell observations were conducted to determine the ideal time point for collecting zygote mRNA. Equal amounts of haploid Hon 1-7 and Pan 2-44 cultures at 10^6 amoebae/ml were spread onto a CMA/2 agar in tissue culture flasks. At time points between 0 and 24 hours, 1 ml of the mating mixture was placed into a microcentrifuge tube and spun at 2,000 RPM for 2 minutes. The supernatant was removed, and the pellet was resuspended in 50 µl of Page's solution and gently vortexed; 10 µl of the resuspended solution was then spread onto a glass slide and the number of zygotes found within

7 minutes were tallied. The observations were performed using a phase contrast microscope under 1000x magnification. Zygotes were determined by morphological differences such as a larger cell size and larger nucleus size relative to haploid cells (Ross 1967). Zygote and amoebae images can be seen in figures 3 and 4.

Figure 3. Microscopic analysis: Image of an amoebae (left) and a zygote (right) taken approximately 18 hours post mating. Cell types distinguished by morphological differences in shape and the size of the nucleus. Scale bar represented by arrows is 50 µm.

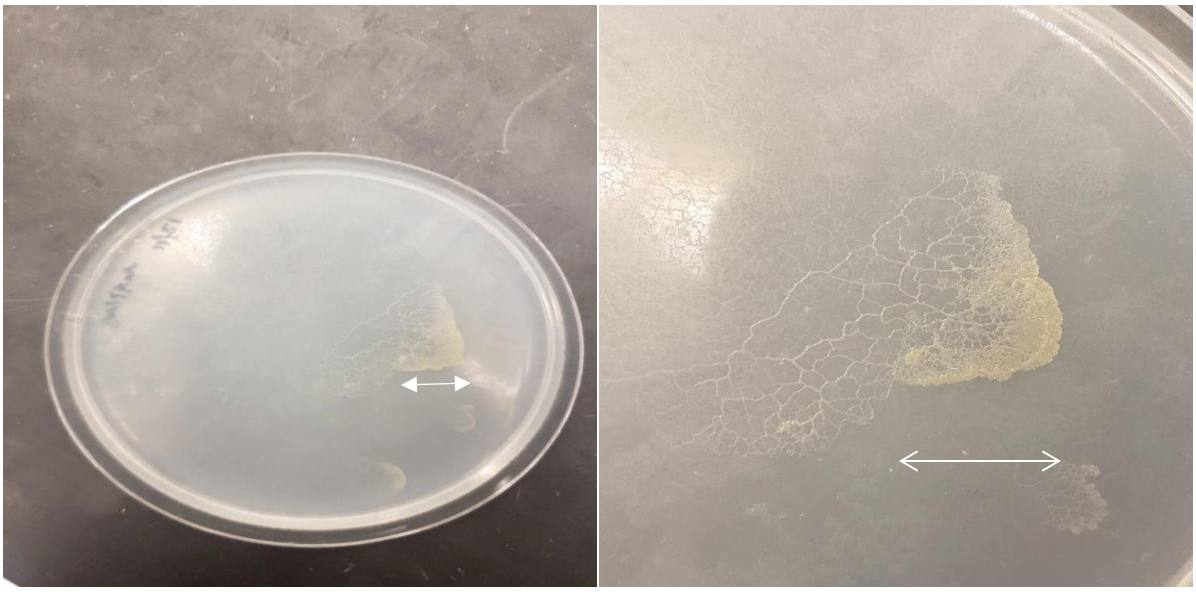

Figure 4. Plasmodia formation: Images of plasmodia formed roughly 6 days post mating. Left image shows the plasmodia to scale on a standard 100mm x 15mm petri plate while the right image is a closer image. Scale bar represented by arrows in 15 mm.

mRNA isolation. – Isolation of amoebal mRNA and zygote mRNA followed standard protocol using the Dynabeads kit (Qiagen, Oligotex Handbook 2012). The specifications used were that of standard mammalian cells. Due to constraints within methodology, zygote mRNA was isolated from a mixture of amoebal cells and young zygotes and was taken roughly 18 hours after mating. Isolation of plasmodia mRNA followed standard protocol using the New England Biolabs Oligo d(T) magnetic bead isolation kit (NE Biolabs, Magnetic mRNA Isolation Kit, 2018).

Generation of cDNA/ purification and amplification of unique transcripts – Prior to cDNA synthesis, mRNA extracted from *D. iridis* was suspended at a higher concentration approximately 2.5 µg/ µl. From the mRNA extracted, cDNA was generated using Takara's SMARTer cDNA synthesis kit (Clontech Laboratories inc. SMARTer™ PCRcDNA Synthesis

Kit User Manual, 2014). The cDNA libraries were then used in Suppressive Subtractive Hybridization which followed that of Clontech® PCR-Select™ cDNA Subtraction Kit protocol (Clontech Laboratories inc. PCR-Select™ Bacterial Genome Subtraction KitUser Manual, 2016). A significant deviation from the protocol included replacing all phenol-chloroform extractions with Takara's zymoclean DNA purification spin columns. This increased the purity and yield of our samples. There was a total of two subtractions; zygote subtracted with amoebae cDNA (sub1; figure 5) and zygote subtracted with plasmodia cDNA (sub2; figure 6). Sample images of our RSA digestion and ligation efficiency gels can be found in appendix A.

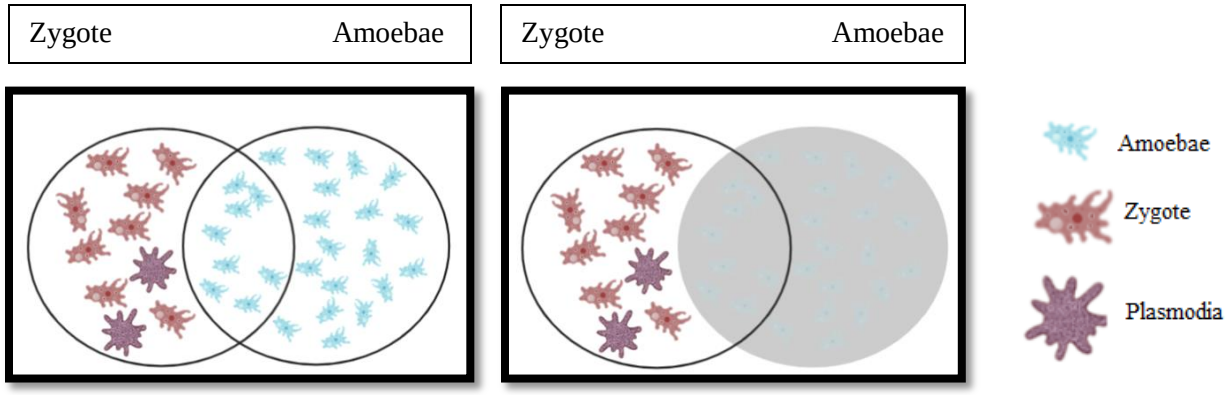

Figure 5. Subtraction 1 (Zp-A). Subtracted cDNA libraries are depicted by Venn diagrams where the left image shows our unsubtracted zygote cDNA library containing zygote, amoebae and plasmodia cDNA. The cDNA shared between the zygote and amoebae cDNA libraries are subtracted away to leave zygote and plasmodia cDNA.

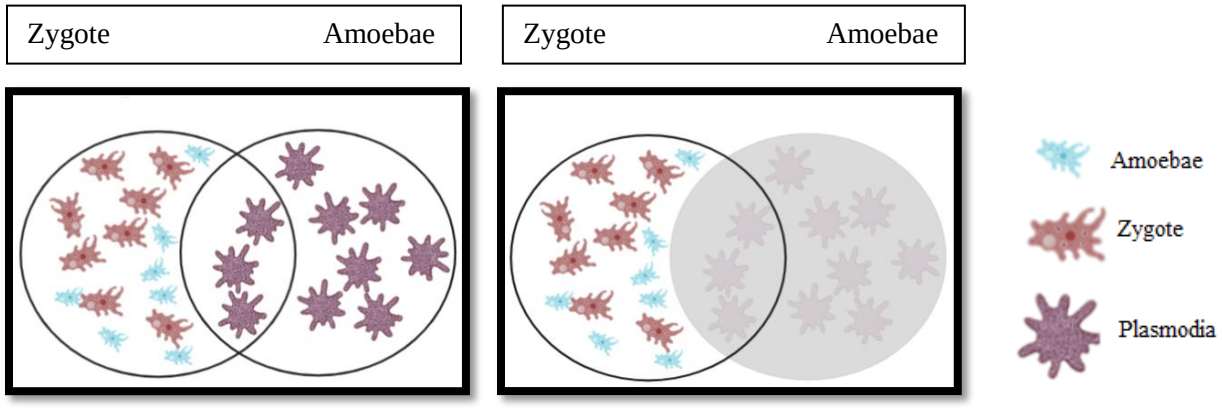

Figure 6. Subtraction 2 (Za-P). Subtracted cDNA libraries are depicted by Venn diagrams where the left image shows our unsubtracted zygote cDNA library containing zygote, amoebae and plasmodia cDNA. The cDNA shared between the zygote and plasmodia cDNA libraries are subtracted away to leave zygote and amoebae cDNA.

TOPO cloning – Approximately 50 ng of subtracted cDNA was placed into a salt solution and mixed with [1/5] pCR 4 or 2.1 plasmids. The TOPO reaction occurred at room temperature for 30 minutes before being placed on ice. The TOPO reaction mix was then pipetted into a vial of TOP 10 OneShot cells and incubated on ice for another 30 minutes to allow plasmid uptake followed by a 30 second 42°C heat shock. The solution was placed back onto ice and 250 µl of SOC media was added to the transformation vial (Invitrogen, One Shot® TOP10 Competent Cells, 2013). The transformation mix was then placed on a shaker in a 37°C incubator for one hour before being spread onto a selection plate containing LB media and ampicillin (100 µg/ ml). The LB/ampicillin plates were incubated overnight, and the resulting colonies were isolated.

Mini preps of E. coli colonies – A single colony was transferred from a selection plate to culture tube containing LB broth and 50 µg/ ml ampicillin. The cultures were incubated overnight at 37°C and shaken at 200 RPM. Sufficient growth was determined by an increased turbidity. Approximately 2 ml of grown culture was transferred into a microcentrifuge tube and spun at

max speed for 2 minutes to create a pellet. The plasmids were purified using Takara's Mini-prep Nucleo-Plasmid kit following standard protocol (Clontech Laboratories inc. Plasmid DNA purification User manual NucleoSpin® Plasmid EasyPure, 2014).

Restriction digest screening – Following plasmid purification, a portion of each sample was digested with *Eco* RI restriction enzyme to verify against false positives, each sample was run onto a 1% agarose gel. A typical digest when imaged consisted of a sharp band around 4,000 bb representing the vector and at least one other band around 100-1,000 bP representing the inserted gene fragment. A sample image can be seen in figure 7.

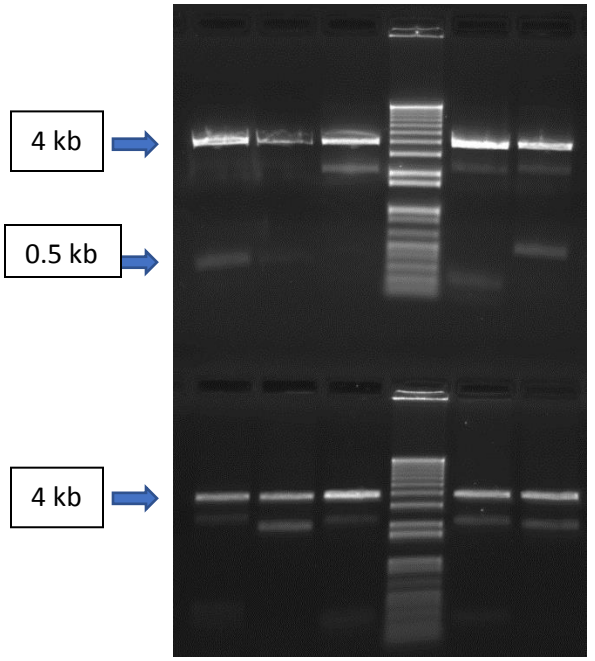

Lane (top)	Clone # DNA
1	343
2	344
3	345
4	1 kb+ marker
5	346
6	348
Lane (bottom)	
1	349
2	350
3	352
4	1 kb+ marker
5	353
6	354

Figure 7. Miniprep from zygote-plasmodia subtraction sample: Various clones were digested with *Eco* RI restriction enzyme to verify successful transformation prior to DNA sequencing. A thick band can be seen at 4,000 bp which represents the cleaved vector DNA while other bands represent *D. iridis* insert DNA. Only clones containing insert DNA were chosen for further analysis.

DNA sequencing setup – Following restriction digest screening, 150 ng of DNA was used along with 320 pmol T7 primer, 1.5 µl [5X] Sequencing Buffer, 1.0 µl Big Dye Terminator version 3.1 sequencing reagent in a final volume of 10 µl. The reaction tubes were placed into a thermocycler for 25 cycles (96°C for 10 seconds, 50°C for 5 seconds, 60°C for 4 minutes). Following the sequencing reaction, samples were precipitated by adding 40 µl Na/EtOH solution and incubated at room temperature for 15 minutes. They were then centrifuged at max speed for 20 minutes at 4°C. The supernatant was removed, and pellet was washed with 250 µl of 70% EtOH and centrifuged on max speed for 5 minutes at 4°C. The supernatant was removed again, and reaction tubes were aspirated at room temperature before being dried under vacuum centrifugation for 2 minutes. Dry pellets were resuspended in 15 µl Hi Dye solution and heated to 95°C for 2 minutes in a dry bath and then cooled before DNA sequencing. The samples were vortexed and stored in the freezer until being placed in the DNA sequencer.

DNA sequencing – All samples were sequenced at DePaul University using an Applied Biosystems 310 DNA sequencer. The sequencer utilizes the Sanger sequencing method which synthesizes DNA fragments with a mixture of dNTP's and fluorescently tagged ddNTP's which terminate further polymerase activity (Sequencher, 2019).

BLAST searches and protein characterization – Sequence data was analyzed using sequencher software. Open reading frames (ORF) were identified and then converted into protein sequences using ExPasy (Bionformatics, Swiss Institute of, 2019). Candidate ORF's were uploaded into NCBI's Genbank database and searched BLASTp with no database constrictions. Nucleotide sequences were searched using BLASTn without any constrictions and BLASTx which was

constrained to amoebozoan and mycetozoan databases. Matches containing the lowest E values were selected while matches with E values higher than 10^{-3} were omitted (Altschul et al. 1990).

DIG labelling and detection – Probes used in Southern and dot blots were labeled and detected according to the protocol from the DIG Labeling and detection kit provided by Roche (Roche inc. DIG DNA Labeling and Detection Kit, 2004). An additional step was added onto the labelling protocol to remove unincorporated nucleotides. Following the DIG DNA labelling step, 4 M LiCl, EtOH and herring sperm DNA was added to the solution before it was frozen at 80°C for 30 minutes. The DIG-labeled samples were then pelleted by centrifugation at 21,460 x g, 4°C for 30 minutes before being resuspended into TE buffer. The probes for the southern blot consisted of differentially expressed genes profilin A (amoebae gene) and fragmin P (plasmodia gene). The probes for the dot blots consisted of amoebal cDNA, plasmodial cDNA, subtracted 1 (zygote minus amoebae cDNA) and subtracted 2 (zygote minus plasmodia cDNA). A labeling efficiency test was performed in order to confirm each of the labeled probes had a sufficient level of DIG labeled nucleotides incorporated within the DNA fragments which can be seen in the appendix B.

Southern blot – Southern blots were made using bi-directional blotting to confirm the success of subtraction generated from the SSH procedure from the protocol of Smith and Summers, 1980. The lanes consisted of unsubtracted tester (amoebae + plasmodial cDNA) sub. 1 (zygote + plasmodial cDNA) and sub. 2 (zygote + amoebae cDNA). The probes consisted of DIG labeled fragmin P and profilin A; DNA from fragmin P and profilin A genes were also added as a positive control for each blot. Each lane had approximately 0.4 µg of DNA.

DNA dot blot – To give us a better indication of differential expression between cell types, four DNA dot blots were created. Each blot consisted of the same clone DNA spot patterns probed with a different DIG-labelled probe. One 1 µl drops (10 ng/µl) were spotted onto positively charged nylon membranes. Cloned DNA at a concentration of 100 ng/ µl was diluted; 1 µl DNA in 9 µl of denaturation solution (4 M NaOH and 100 mM EDTA) and then incubated at room temperature for ten minutes prior to spotting. Once all the samples were added to the membrane the DNA was fixed using a DNA crosslinker. The membranes were then hybridized and detected using the DIG Labeling and detection kit protocol provided by Sigma Aldrich (Roche, 2004).

RT-PCR - RT-PCR was performed using the protocol from Invitrogen RT-PCR kit (Invitrogen, SuperScript™ III One-Step RT-PCR System with Platinum™Taq DNAPolymerase, 2016). mRNA from amoebae, zygote (containing some amoebae) and plasmodia were used as template while primers were specifically designed to flank the sequences of each clone. The presence or absence of a PCR product along with the intensity of the band correlates to how abundant the genes are within a population of mRNA.

Results and discussion:

Determination of timepoint selection:

Haploid strains were spread in equal amounts onto a CMA/2 agar cell culture flask. The strains Hon 1-7 and Pan 2-44 were chosen due to a previous study which provided evidence for a fast mating time and a near equal mitochondrial donation in progeny (Scheer and Silliker 2006). The agar culture flasks were allowed to incubate at room temperature for 18 hours. This timepoint was chosen because it yielded the highest number of zygote cells without containing any observed microplasmodia which consist of 2 or more nuclei per cell (figure 8).

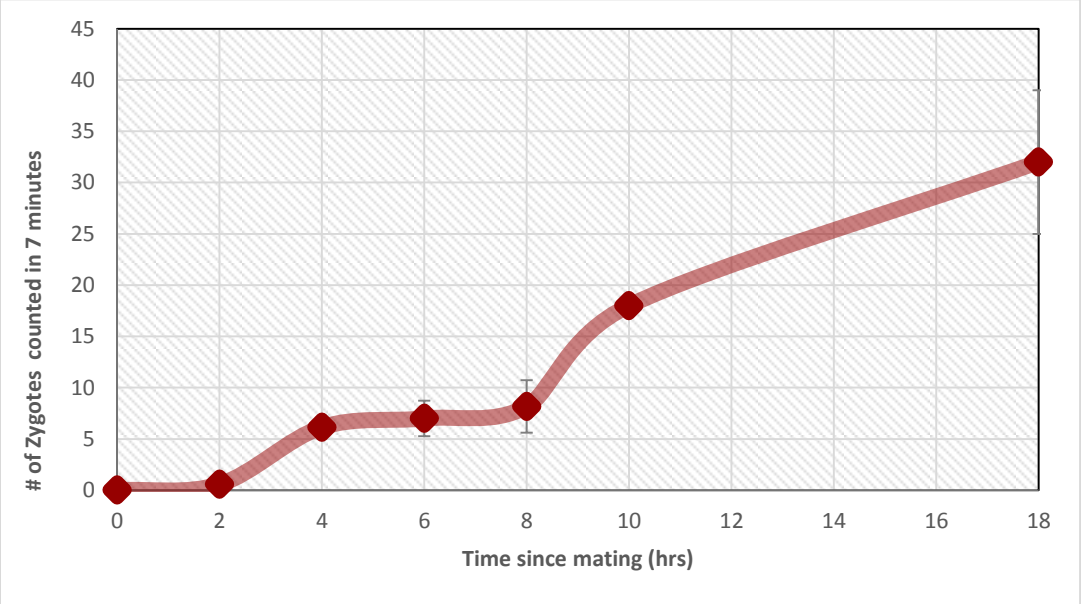

Figure 8. Time point selection: The number of zygotes were counted for 7 minutes under 1000x magnification. The number of replicates varied between different timepoints where hours 0, 2 and 4 have n=7; hour 6 has n=5, hour 8 has n=6, hour 10 has n=1 and hour 18 has n=2.

Southern blot analysis:

Southern blot were conducted to confirm successful subtractions. Evidence of successful subtraction 1 would be indicated by removal of amoebal genes, in this case profilin A. This would show hybridization in the unsubtracted DNA lane but not in any others. Evidence of a

successful subtraction 2 would be indicated by the lack of hybridization of profilin A in the sub. 2 lane while a hybridization of fragmin P in all of the experimental lanes (figure 9).

Unsubtracted tester sub. 1 contained genes from amoebae, zygote and plasmodia. Sub. 1 contained genes from zygote and minimal plasmodia subtracted with amoebal cDNA which will be referred to as Zp(-A). Sub. 2 contained genes from zygote and minimal amoebae subtracted with plasmodial cDNA which will be referred to as Za(-P). The probes chosen were fragmin P and profilin A, both of which are expressed at distinct stages in the *D. iridis* life cycle (T'Jampens et al. 1999) making them useful probes to identify differential expression. DNA from fragmin P and profilin A were also loaded onto the blot as positive controls.

Upon detection with the fragmin P probe, bands appeared in all the lanes except for the lane containing profilin A, indicating that there are plasmodial genes present in all three experimental samples. This was expected as all of the libraries used contained zygote genes which are essentially early plasmodia genes. Upon detection with the profilin A probe, bands appeared only in the unsubtracted tester cross 1 and profilin A lanes. This was also expected because the unsubtracted sample contained cDNA from amoebae and zygote stages before being subtracted with amoebae. The disappearance of amoebal genes from unsubtracted cross 1 to subtracted 1indicated a successful subtraction by the removal of an amoebae specific genes.

Probe: Fragmin P	Probe: Profilin A

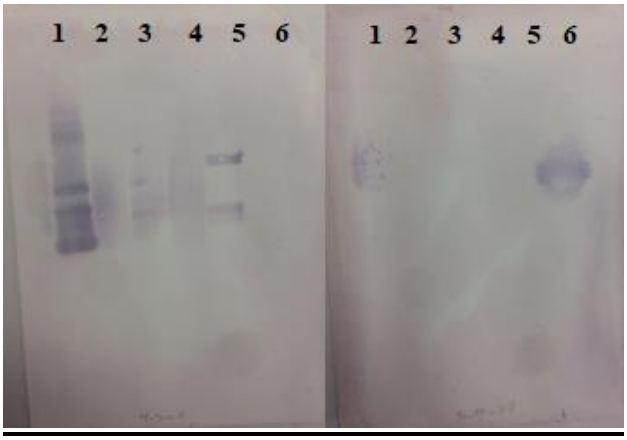

Lane (left)	Clone DNA
1	1 kb marker
2	Unsubtracted tester Zpa
3	Tester sub. 1; Zp(-A)
4	Tester sub. 2; Za(-P)
5	Fragmin P
6	Profilin A

Lane (right)	Clone DNA
1	Unsubtracted tester Zpa
2	Tester sub. 1; Zp(-A)
3	Tester sub. 2; Za(-P)
4	1 kb marker
5	Fragmin P
6	Profilin A

Figure 9. Southern blot of differentially expressed genes: A southern blot was performed in duplicate yielding consistent results; the best blots were included in this report. The left blot was probed with DIG labeled fragmin P while the right blot with DIG labeled profilin A. The 1kb marker in the fragmin P blot reacted with the probe along with the experimental subtractions. Reaction with the marker is likely due to cross reaction between the fragmin P cloning vector and the vector sequences in the marker. This is not uncommon and does not have any bearing on our results.

Overview of Clone characterization:

A total of 200 clones were sequenced yielding 183 contigs with reliable sequence accuracy. These 183 contigs were analyzed for homology matches and searched against the Genbank gene database while contigs with fewer than 100 bp or contigs that had no detectable open reading frames (ORFs) were omitted from analysis. The clones were broken into categories based on their known or predicted protein function and can be seen in Table I. Hypothetical proteins are clones that matched sequences within the Genbank database but did not have a function associated with them while unknown function denotes clones that did not match anything in the database.

Table I: Overview of clones broken by cellular function

Cellular function	# of clones found
Cytoskeleton	12
Mitochondrial Inheritance	4
Ubiquitin-Proteasome	9
Signal Transduction	22
Hypothetical Proteins	15
Metabolic/ housekeeping	68
Unknown	53

Cytoskeleton proteins:

Various cytoskeletal proteins were uncovered from our subtractions, in particular proteins involved in the cytoskeletal makeup or composition. These proteins can be seen in Table II. Differentially expressed cytoskeleton proteins were expected to be found based on previous literature (Bailey et al. 1992). It is interesting to note that many of these proteins showed a high degree of similarity to unrelated organisms, indicating a high level of conservation. Fragmin P (clone #33) was the only characterized protein we uncovered that has been experimentally studied in myxomycetes (T'Jampens et al. 1997). Interestingly enough, this protein did not appear to have stage specific expression in the dot blots but does in the Southern blots. One explanation could be that the fragmin domain is highly conserved between fragmin P (plasmodial specific) and fragmin A (amoebae specific). This would generate a signal from every probe used in our experiments as they all contain some isotype of fragmin. Upon characterization through the GenBank database, clone #33 did in fact match both fragmin P and fragmin A but was identified as fragmin P based on the subtraction (amoebae subtracted away) as well as a lower E value associated fragmin A. Nevertheless, it is likely this gene represents fragmin P which hybridizes to both isoforms of fragmin. The same concept can be said about isoforms of profilin hybridizing with our profilin A probe.

Previous studies have identified various cytoskeletal isotypes that are stage specific in *P. polycephalum*. Our dot blot results do not support stage specific expression of the tested cytoskeletal proteins in *D. iridis.* Both cytoskeleton structural and organization proteins appear to be continuously expressed between both the amoebae and plasmodial stages. This was a surprise due to evidence for differential expression of cytoskeletal proteins found in *P. polycephalum* (Bailey et al. 1992).

Two explanations for the continuous expression observed in the dot blot data is that the cytoskeletal proteins are the same across cell stages or that the probe does not differentiate between different isoforms due to a high level of conservation. If the genes encoding plasmodial and amoebal cytoskeletal proteins are very similar, then one isoform would hybridize with its counterpart despite being differentially expressed. This was believed to be observed in both the fragmin P and profilin A genes blotted. It is possible that the cytoskeletal proteins we blotted could have given rise to false positives if the sequence similarity between the isotypes in amoebae and plasmodia is high. Also, it is possible that the organizational composition may change between amoebal and plasmodial stages and not be truly differentially expressed. For example, the ratio of a given cytoskeletal protein may change between the stages despite being expressed in both. This would yield a continuous expression in a dot blot regardless of whether the compositional makeup of the cytoskeleton is changing.

Lastly, a final explanation for the lack of differentiation could be that cytoskeletal proteins are encoded by the same genes between amoebae and plasmodial cell stages but could contain post translational modifications that distinguish between the two isotypes. This would mean genes like profilin or fragmin are encoded by the same genes but are modified according to the life cycle stage in which the organism is in. It is possible that we isolated stage specific

cytoskeletal ORF's that cross react with its isotype counterpart. This cross reaction would explain the continuous expression for genes such as fragmin P which are known to be stage specific.

Table II: Cytoskeletal proteins

Clone # (ORF size)	Protein shared domain	Organism overlapped	E value	Possible function
23/ 80 (461 /464 BP)	Myosin binding protein C	*Homo sapiens*	1e-89	Heart muscle development
33[i] (593 BP)	actin-binding protein fragmin P	*Physarum polycephalum*	2e-80	Cytoskeletal protein
73 (828 BP)	Beta actin (NBD_sugar_kinase_HSP70_actin family)	*Didymium squamulosum*	4e-154	Cytoskeleton, plasmodia development
77 (541 BP)	Actin	*Physarum polycephalum*	6e-96	Cytoskeleton, plasmodia development
180 (262 BP)	CAP-Gly containing linker protein 1	*Equus caballus*	4e-37	Microtubule rearrangement
321/ 325/ 360 (322/ 333/ 322 BP)	ADP-ribosylation factor (ras_superfamily)	*Heterostelium album*	2e-55/ 1e-37/ 4e-54	GTP domain protein, involved in vesicle transport and actin remodeling
324 (126 BP)	tubulin polymerization-promoting protein family member 3	*Oryzias latipes*	4e-12	Cytoskeletal proteins; microtubule bundling/ formation
326/ 327 (311/ 306 BP)	pericentrin	*Homo sapiens*	4e-95/ 2e-88	Mitotic spindle organization, possibly involved in cell cycle progression

[1] Colors used to represent evolutionary lineages where green is mycetozoan and blue is amoebozoan

Suspected mitochondrial inheritance proteins:

Our initial goal was to uncover genes involved in mitochondrial inheritance which based on observation, exert their effect in the zygote (Moriyama et al. 2005, Moriyama et al. 2010). Among the genes we expected to uncover were nucleases, DNA packaging proteins and shuttle proteins involved in the transport of nucleases into the mitochondria (Itoh et al. 2011). Of the proteins with characterized functions, we identified two strong and one weaker candidate to be involved in mitochondrial inheritance. These can be seen in Table III. Our dot blots suggest that

clones #148 and #174 have a strong bias toward zygote gene expression based on their relative intensities to the subtracted probes versus the amoebae and plasmodial probes. Due to the lack of genetic information available on selective degradation of mtDNA in myxomycetes the proteins deemed as suspected in mitochondrial inheritance cannot be conclusively attributed to be involved in this mechanism. These proteins do however offer an intriguing possibility for the uniparental inheritance of myxomycete mtDNA.

Lysis protein E/ scaffolding protein D was uncovered in overlapping clones #148/209 within the first subtracted library. Both lysis protein E and scaffolding protein D had nearly identical matches on BLASTp which is why they are both included in the characterization of clones #148 and #209. Lysis protein E was identified as a viral protein which functions to inhibit enzymatic activity of lipid synthesis. It is used by viruses to inhibit bacterial membrane synthesis and induce lysis of the cell (Uniprot P03639, 2019**)**. Scaffolding protein D's typical function is to pack viral DNA into mature capsids, indicating that it may have DNA binding and packaging abilities (Uniprot P69487, 2019). With respect to mitochondrial inheritance in myxomycetes, it is possible these proteins could have analogous functions to package mtDNA or inhibit lysis of mitochondrial membrane.

Another candidate for selective degradation of mtDNA is replication-associated protein A represented by clone #174. This protein has a zinc finger motif and possesses both DNA binding and endonuclease activity. When bound to dsDNA this protein can prevent hydrolysis from nuclease activity making it a strong candidate for both selective degradation and preservation of mtDNA (Uniprot P03631, 2019). In theory, this clone represents a protein capable of performing selective degradation by cleaving unwanted mtDNA and proliferating desirable mtDNA by protecting it from hydrolytic endonuclease activity.

Lysis protein E, scaffolding protein D (clones #148/209) and replication associated protein A (clone #174) may represent novel myxomycete genes generated through viral horizontal gene transfer. Similar processes of horizontal gene transfer have been identified from viral to bacterial genomes (Lekunberri et al. 2017), involving a study which provides evidence of the transfer of antibiotic resistance genes from virus to bacteria. Myxomycetes are exposed to bacteriophages naturally by ingesting infected bacteria which could expose the organism to many viral genomes. Due to the differences in life strategies between myxomycetes and viruses it should be concluded that the proteins likely do not have the exact same functions in the two organisms. It is possible that *D. iridis* may have acquired genes from viral DNA which over time evolved to carry out selective degradation of mtDNA.

Table III: Suspected mitochondrial inheritance proteins

Clone # (ORF size)	**Protein shared domain**	**Organism overlapped**	**E value**	**Possible function**
7 (283 BP)	Ribonuclease E (RNase E_G_superfamily)	*Saccoglossus kowalevskii*	4e-05	Nuclease activity, cleaves ssRNA
148/ 209 (177/ 173 BP)	Lysis protein E, external scaffolding protein D	*Xanthomonas citri*, Numerous enterobactericiae phages	3e-31, 3e-29	Induce cell lysis by inhibiting lipid synthesis
174 (248 BP)	Replication-associated protein A	*Escherichia coli* bacteriophage	3e-59	Viral DNA replication; properties prevent hydrolysis by nucleases and DNA rep. prevention

Ubiquitin-proteasome proteins:

A total of 8 proteins involved in the ubiquitin-proteasome pathway were uncovered from our SSH crosses and can been seen in Table IV. This was surprising since evidence for ubiquitin-proteasome proteins have not previously been identified as being involved in zygote or

plasmodial development. Our dot blot experiment revealed 3 of the clones (#88, #332 and #366) to have a bias expression in plasmodia or amoebae cell types. It remains unclear if the ubiquitin-proteasome proteins we obtained are stage specific or if they provide a specialized role in the amoebae-zygote transition.

One explanation for the increase of ubiquitin-proteasome proteins could be that during zygote development there is a need for the cell to recognize and degrade amoebae specific proteins. We know based on previous research that roughly 5% of genes are stage specific (T'Jampens et al. 1999) indicating that there may exist a plethora of amoebae specific proteins no longer needed for the cell. It would be advantageous for the cell to recycle these proteins by means of the ubiquitin-proteasome pathway.

Another explanation for the increase of ubiquitin-proteasome proteins could simply be in correlation to an increase of protein synthesis in general. Roughly 1 in 4 proteins synthesized are done so incorrectly and therefore get tagged for degradation (Zientara-Rytter and Subramani 2019). During the zygote's extended cell cycle there is a higher rate of protein synthesis than at any other point within its life cycle (Turnock et al. 1981). This suggests an increase in protein synthesis occurs during zygote development. The sheer increase in protein synthesis could indicate a functional need for the increase in ubiquitin-proteasome protein synthesis to mitigate improper folding of various other proteins synthesized at this stage.

Table IV: Ubiquitin-proteasome proteins

Clone # (ORF size)	Protein shared domain	Organism overlapped	E value	Possible function
63[i] (684 BP)	Ubiquitin 4 (Ubq_superfamily)	*Physarum polycephalum*	6e-149	Proteostasis
88 (528 BP)	Ubiquitin 4 (ubq superfamily)	*Physarum polycephalum*	8e-60	Ubiquitin proteasome pathway
144 (235 BP)	Ankyrin repeat and SOCS box containing-8	*Homo sapien*	0.0 – 1e-180	Ubiquitination/ protein degradation
151/ 195 (257/ 344 BP)	SAM-dependent methyl transferase (AdoMet_MTases_superfamily)	*Acidobacteria bacterium*	2e-39/ 4e-50	Methyl transfers/ ubiquitination probably
153 (254 BP)	Histidine kinase	*Candidatus Fermentibacteria*	3e-32	Signal transduction
164 (354 BP)	26s proteasome regulatory sub unit 4 homolog A-like	*Chenopodium quinoa*	3e-71	Degrades misfolded/ ubiquitinated proteins
197 (187 BP)	Ubiquitin-ligase like protein	*Tilletiopsis washingtonensis*	3e-39	Involved in UBQ pathway, possible transfer or recruitment of UBQ ligase
332 (127 BP)	BTB/POZ domain containing protein	*Acanthamoeba castellanii*	3e-12	Likely acts as a substrate specific adapter to E3 ubiquitin ligase
366 (508 BP)	Cullin 3	*Dictyostellium discoideum*	2e-92	Involved in ubiquitin protein ligase binding

[i] Colors used to represent evolutionary lineages where green is mycetozoan and blue is amoebozoan

Signal transduction proteins:

An irreversible developmental switch occurs during zygote formation which allows for the transformation of haploid amoebae into diploid zygotes. Plasmodia form from subsequent rounds of mitosis or by the fusion of other genetically identical zygotes or plasmodia. During the amoebae-plasmodia transition, the cell must be able to regulate changes in gene expression in a relatively short amount of time. The cell uses intracellular signal transduction to turn on plasmodial specific developmental pathways and turn off amoebae specific pathways.

Little is known about signal transduction in myxomycetes as it pertains to zygote development. We tested 11 signal transduction genes in our blots and observed 7 appearing to show a biased expression toward zygote or plasmodial cell types. The genes consisted of GTPase

domain proteins, transmembrane proteins, kinase domain containing proteins and other signal transduction elements (see table V).

We uncovered two transcription factors in our subtractions and tested them on our dot blots; this included sry-box protein 9 (clone #314) and tetrapeptide repeat homeobox (clone #171/ 189). Neither of the transcription factors showed a biased expression toward a cell stage based on our dot blot data. This did not meet predictions, as we expected to uncover plasmodial specific transcription factors. One explanation for the low number of transcription factors uncovered could be that transcription factors, when expressed, are done in low levels making them challenging to find. It is probable that transcription factors responsible for the amoebal-plasmodial transition exist but were not found in this study.

Table V: Signal transduction proteins/ transcription factors

Clone # (ORF size)	Protein shared domain	Organism overlapped	E value	Possible function
150[i] (336 BP)	LIM-type zinc finger-containing protein/ arrestin domain-containing protein	*Dictyostellium discoideum*	3e-40	Signal transduction, vacuole organization
159 (308 BP)	hexose phosphate transport system regulatory protein	*Planoprotostelium fungivorum*	7e-27	Transmembrane protein involved in signaling
166 (196 BP)	GPN-loop GTPase 2	*Cavenderia fasciculata*	1e-18	GTPase activity
167 (150 BP)	EGF like domain	*Tieghemostelium lacteum*	1e-09	Cell signaling, membrane receptor
171/ 189 (292/ 292 BP)	Tetrapeptide repeat homeobox 1	*Numida meleagris*	7e-06/ 7e-06	Encode DNA binding proteins/ development
184 (436 BP)	RapGAP/RanGAP domain-containing protein	*Heterostelium album*	5e-81	GTPase activity activator, possibly developmental
207 (164 BP)	S-layer homology domain-containing protein	*Paenibacillus agaridevorans*	1e-04	Associated with cell wall, possibly structure or signaling
208 (282 BP)	ras-related C3 botulinum toxin substrate 1-like	*Acanthaster planci*	2e-60	G-protein activity, signal transduction and growth
211 (793 BP)	Troponin L1	*Homo sapiens*	2e-132	Skeletal/ heart muscle protein
215/ 216b (337/ 337 BP)	Armadillo-type protein, Elongation factor 3	*Lobosporangium transversal, Ortierella verticillata*	9e-16, 7e-16	Interacts with DNA and usually binds to it or large proteins (ex. Helicases, ATPases) EF-3 is a protein

				involved in ribosome synthesis
314 (250 BP)	Sry-box protein 9	*Eptatretus burger*	7e-12	Transcription factor that controls many development processes
329 (142 BP)	Protein phosphatase 2C domain	*Acanthamoeba castellanii*	7e-07	Cell signaling/ kinase activity
333 (275 BP)	cystathionine-beta-synthase domain-containing protein	*Acanthamoeba castellanii*	8e-15	Regulates enzymatic activity
353 (109 BP)	RHS repeat-associated core domain-containing protein	*Alloactinosynnema album*	4e-10	Highly conserved, many involved in secreted toxins or intercellular signaling
369 (113 BP)	FYN/Yes-like tyrosine-protein kinase	*Planoprotostelium fungivorum*	1e-14	Intracellular signaling/ tyrosine kinase activity
371 (359 BP)	protein serine/threonine kinase (PKC_like_superfamily)	*Tieghemostelium lacteum*	2e-84	Cell signaling which effects metabolism, proliferation, growth
386 (190 BP)	Rab GDP dissociation inhibitor alpha (NADB_Rossman_superfamily)	*Cavenderia fasciculata*	2e-33	Regulates the GDP/GTP exchange of Rab proteins by inhibiting dissociation of GDP
390 (89 BP)	GCN20-type ATP-binding cassette protein GCN3, putative (SunT_superfamily)	*Entamoeba invadens* IP1	1e-04	Transmembrane transporter
391 (111 BP)	putative protein serine/threonine kinase (PKc_like_superfamily)	*Cavenderia fasciculate*	1e-12	Intracellular signaling kinase activity, possible cytoskeleton affiliation
398 (371 BP)	sugar-binding protein & RHS repeat-associated core domain-containing protein	*Alloactinosynnema album*	8e-07	Intercellular signaling

[i] Colors used to represent evolutionary lineages where green is mycetozoan and blue is amoebozoan

Proteins with unknown function and hypothetical proteins:

Of the 183 contigs characterized into protein ORF's, 45 either matched only hypothetical proteins, or did not match any sequences in GenBank. This yielded 30 individual hypothetical or unmatched proteins after assembly of overlapping sequences. Due to the lack of myxomycete bioinformatics available about 29% of our sequenced libraries could not be characterized into known protein ORF's despite having high quality sequencing reads. It is interesting to note that clones #21/162/178, #188, #194, #312, #313, #340, and #399 only matched hypothetically proteins belonging to the mycetozoa phylum or related amoebozoa. These contigs could indicate proteins novel to the mycetozoa taxa, as they don't match any organisms outside of this lineage.

We chose 13 unknown clones to test in our dot blots and limited our inclusion criteria to the largest ORF sizes along with matches to mycetozoan organisms. These clones can be found in table VI. Of the 13 proteins tested, 7 of them showed a biased expression toward zygote or plasmodial cell types (see dot blot analysis discussion). These clones could represent novel mycetozoan genes and appear to be regulated during zygote development.

Table VI: Hypothetical proteins

Clone # (ORF size)	**Protein shared domain**	**Organism overlapped**	**E value**	**Possible function**
21/ 162/ 178 (700 BP)	Hypothetical protein, DOC2	*Sphaeroforma arctica*, Piromyces	1e-29	"Extracellular serine rich", homolog is Ca^{2+} dependent and used in exocytosis
97[i]	hypothetical protein, SNF2-related domain-containing protein	*Cavenderia fasciculate*	1e-9, 5e-6	Microtubule organization or mitotic process
188 (360 BP)	Hypothetical protein	*Acanthamoeba castellanii*	2e-46	Many hits to myxomycetes, possibly specific to the phylum
191 (186, 178 BP)	Hypothetical protein	*Stigmatella aurantiaca, burkholdia*	8e-14, 5e-13	Both organisms seem to have high resistance to antibiotics
194 (121 BP)	Hypothetical protein	*Planoprotostelium fungivorum*	3e-04	
215/ 216a (337/ 337 BP)	Hypothetical protein	*Planoprotostelium fungivorum*	3e-21	
312 (101 BP)	Hypothetical protein	*Acytostelium subglobosum*	1e-09	-
313 (190 BP)	Hypothetical protein	*Planoprotostelium fungivorum*	4e-03	
399 (500 BP)	hypothetical protein	*Dictyostelium discoideum*	4e-16	

[i] Colors used to represent evolutionary lineages where green is mycetozoan and blue is amoebozoan

DNA binding proteins:

Three proteins of interest were identified as having DNA binding domains, which are valuable in identifying developmentally related genes because they possess key characteristics of both nucleases and transcription factors (Table VII). Due to the timing of zygote extraction and the nature of DNA binding proteins' cellular function, these clones represent genes with a high probability of plasmodial development functions. It should also be noted that clones #148/209 are also included as mitochondrial inheritance proteins. This was necessary because the clones had two different ORF's containing low E-values.

Table VII: DNA binding proteins

Clone # (ORF size)	Protein shared domain	Organism overlapped	E value	Possible function
148/ 209[i] (120/ 116 BP)	DNA Binding protein	*Salmonella enterica*	1e-15, 6e-15	DNA binding domain
345 (116 BP)	DNA Binding Protein	Pedobacter sp.	1e-15	DNA binding domain
394/ 401$_i$ (546 BP)	RGS-containing protein kinase RCK1	*Cavenderia fasciculate*	7e-12	Kinase Domain, Zinc Finger

[i] Colors used to represent evolutionary lineages where green is mycetozoan and blue is amoebozoan

Dot blot analysis:

Dot blots (figures 10-13) were conducted to determine differential expression between plasmodial and amoebal cell types. A clone map is included in Table VIII. The level of intensity was scored by four individuals working in the Silliker lab and averaged (Table IX). A value of 0 represents no signal while values 1-5 represent various intensities with 5 being the strongest signal observed on the blot. By using subjective scoring, it was possible to compare differential expression between the blots. An assessment for biased gene expression was attributed to amoebae, plasmodia or zygote. A clone was scored "n/a" if the intensity was minimal or showed no difference between probes. Biased expression was determined based on the relative intensities

each gene displayed in the various blots. A strong signal in the subtracted libraries compared to amoebae appears biased toward plasmodial or zygote gene expression while relatively consistent intensities was determined to be continuously expressed, or n/a. Out of the 48 genes blotted, 21 appeared to exhibit differential gene expression. These are genes we believe to be expressed early during zygote development and could play a role in zygote differentiation and plasmodial development.

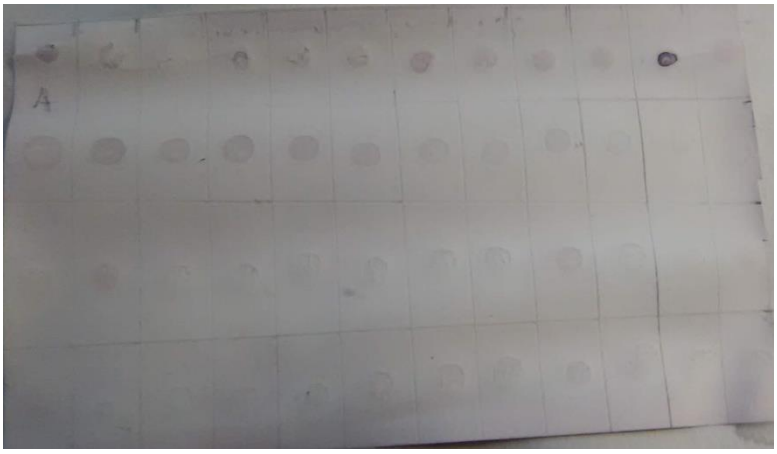

Figure 10. Dot blot probed with amoebal cDNA: Competent amoebae mRNA was extracted and converted to cDNA where it was then labeled and hybridized following the DIG hybridization protocol.

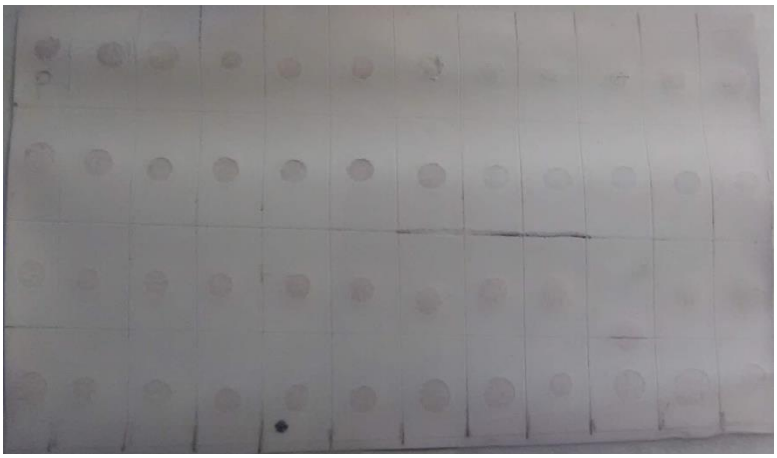

Figure 11. Dot blot probed with plasmodial cDNA: Plasmodial mRNA was extracted and converted to cDNA where it was then labeled and hybridized following the DIG hybridization protocol.

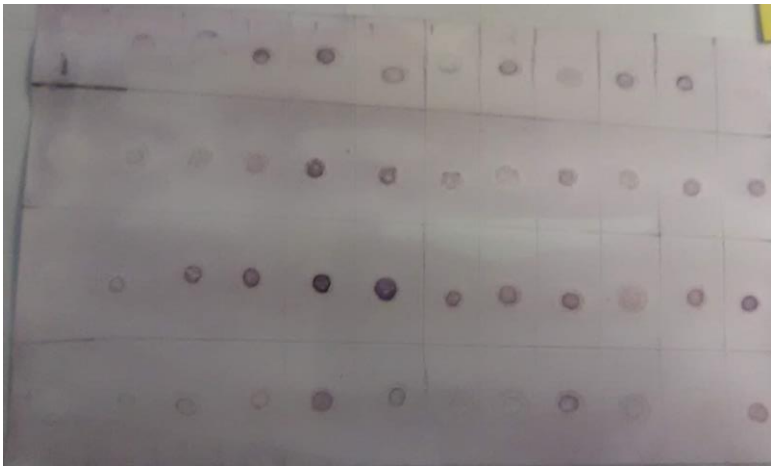

Figure 12. Dot blot sub 1, Zp(-A) probe: The subtracted library from sub. 1 was digested with RSA I for 1.5 hours prior to labelling to remove adapter sequences. The library was then labelled and hybridized using the DIG hybridization protocol. Darker clone spots indicate clones enriched in the subtracted library.

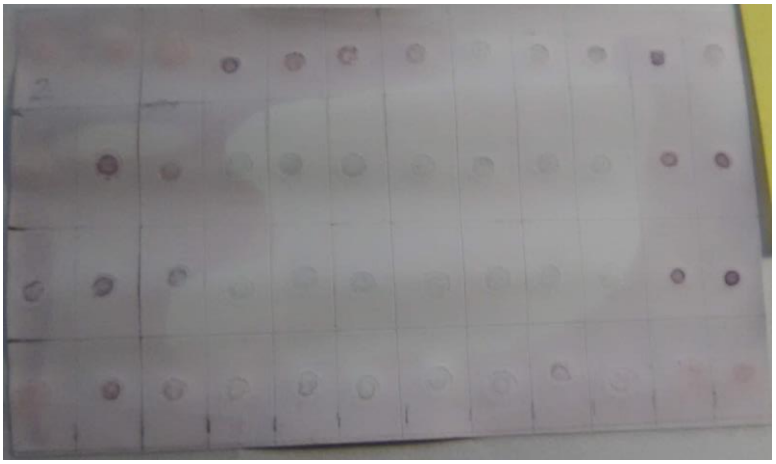

Figure 13. Dot blot sub. 2, Za(-P) probe: The subtracted library from sub. 2 was digested with RSA I for 1.5 hours prior to labelling to remove adapter sequences. The library was then labelled and hybridized using the DIG hybridization protocol. Darker clone spots indicate clones enriched in the subtracted library.

Table VIII: Dot blot clone map:

	1	2	3	4	5	6	7	8	9	10	11	12
A	-	#63	#88	#144	#195	#164	#197	#332	#365	#23	#33	#73
B	#97	#171	#180	#184	#314	#324	#326	#17	#150	#7	#148	#174
C	#394	#331	#153	#167	#207	#208	#211	#329	#336	#369	#371	#28
D	#145	#157	#163	#168	#213	#219	#399	#307	#14	#361	#370	#193

Table IX: Consolidated dot blot clone list

Clone #	*Pos.*	Gene	Am	Zp(-A)	Pl	Za(-P)	Biased Expression
-[i]	***A1***	Profilin A	3.25	0	3	0.5	n/a
63	***A2***	Ubiquilin 2	2	1	3	0.5	n/a
88	***A3***	Ubiquilin 1	0.75	1	2.5	0.5	Plasmodia
144	***A4***	Ankrin repeat/ SOCS box protein	2.75	3.5	3	3.25	n/a
195*[ii]	***A5***	SAM- dependent methyl transferase	1.75	3.75	2.75	2.25	n/a
164	***A6***	26s 41 proteasome regulatory subunit	1.75	2.5	2.75	2.25	n/a
197	***A7***	Ubiquitin- ligase like protein	3.5	1.25	2.25	2	n/a
332	***A8***	BTB/POZ containing protein	1.75	3.25	1	1.25	Plasmodia
365	***A9***	Cullin 3	2.25	1.5	1	1.5	Slight amoebae
23*	***A10***	Myosin binding protein C	2	3.25	1	2	Plasmodia
33	***A11***	Actin-binding fragmin P	5	3.5	1.75	4.25	n/a
73	***A12***	Beta actin	1.5	0.25	1.5	2.25	Zygote
97	***B1***	NIMA related protein kinase	2	0	1.75	1	n/a
171*	***B2***	Tetrapeptide repeat homeobox	3	1.25	2.5	3.5	n/a
180	***B3***	CAP-Gly containing linker protein	2.25	1.25	3	2.25	n/a
184	***B4***	RapGAP/ RanGAP protein	3	1.5	3	2.5	n/a
314	***B5***	Sry-box protein 9	3	3.5	3.25	2.75	n/a
324*	***B6***	Tubulin polymerization-promoting protein	2.25	2.75	3.25	2.5	n/a
326*	***B7***	pericentrin	2	2	3	1.75	n/a
17	***B8***	Elongation factor 1 (control)	1.25	1.5	1.75	2	n/a

150	***B9***	LIM-type zinc finger protein	1.75	2.75	1.25	1.5	Plasmodia
7	***B10***	Ribonuclease E	1	1.75	1.25	1.25	n/a
148*	***B11***	Lysis protein E/ external scaffolding protein D3	0.75	3	1.5	3.25	Zygote
174	***B12***	Replication- associated protein A	0.25	3	1.25	4.25	Zygote
394*	***C1***	Kinase domain/ zinc finger protein	0.5	0.5	1.5	2.25	Zygote
331	***C2***	Inhibits serine proteases/ toxin	1.5	2	1.5	3.25	Zygote
153	***C3***	Histidine kinase	0.75	2.25	2	2.5	Zygote/ plasmodia
167	***C4***	EGF-like domain protein	1	3.25	2	2.25	Zygote/ plasmodia
207	***C5***	S-layer homology domain protein	0.75	5	2.25	2.75	Zygote/ plasmodia
208	***C6***	Ras-related C3	1	4.75	2	3	Zygote/ plasmodia
211	***C7***	Ras/ GTPase domain protein	1	3.25	1.75	2	Zygote/ plasmodia
329	***C8***	Protein phosphatase 2C domain	1	3.25	1.75	2	Zygote/ plasmodia
336	***C9***	Rab1 family GTPase	1.75	3.25	1.25	2.25	Zygote/ plasmodia
369	***C10***	FYN/Yes-like tyrosine kinase	0.5	2	1	1.5	Plasmodia
371	***C11***	Protein serine/ threonine kinase	0	3.25	0.75	4	Zygote
28	***C12***	-	0.25	4	1	4.25	Zygote/ plasmodia
145	***D1***	-	0.25	0.25	1.75	1	n/a
157	***D2***	-	1	1.25	2	3.25	Zygote
163	***D3***	-	0.25	1.25	2.5	2.25	Zygote/ plasmodia
168	***D4***	-	0.5	1.25	2.75	1.5	Plasmodia
213	***D5***	-	1	3	2.5	2.25	Zygote/ plasmodia
219	***D6***	-	1.25	2.25	2.75	2	n/a
199	***D7***	-	1.25	1	2.5	2	n/a
307	***D8***	-	1.25	1	2	2	n/a
14	***D9***	-	1.5	2.25	1.75	3	Zygote/ plasmodia
361	***D10***	-	1	1.25	1.75	1.75	n/a
370	***D11***	-	0.25	0	1	1.25	n/a
193	***D12***	-	0.25	3	1	2	Plasmodia

[i] colors represent different functional groups of the clones where blue is ubiquitin, orange is cytoskeleton, yellow is miscellaneous, green is signaling, and purple is unknown.

[ii] * represents clones that had at least one other clone assembled in a contig.

Scores are an average of 4 independent analyses done in the Silliker lab.

The results of the dot blots scoring suggest that some of the genes may be differentially expressed but not all. Further testing such as RT-PCR should be done to determine differential

expression of these clones. Characterization based on database searches includes clones not included within the dot blots as well as ones that were represented. After characterization, protein homologs were grouped according to their known or predicted cellular function. The groups include developmental and cytoskeletal, mitochondrial inheritance, ubiquitin-proteasome, signal transduction, DNA binding and unknown. Clones related to metabolic, housekeeping or miscellaneous functions have been omitted from the results and discussion section. Appendix C contains a complete list of the ORFs analyzed.

RT-PCR:

To verify differential expression, we performed an additional assay with clones that yielded no matches to the Genbank database. Three mRNA libraries were selected as templates to be tested with RT-PCR using primers designed specifically to flank the sequences of each clone. The mRNA libraries used were amoebae, zygote (containing some amoebae and plasmodia), and plasmodia. The differences of band intensity seen in the PCR products is associated with the level of gene expression seen at each stage for a particular clone (figures 14 and 15). Clones #14, 58, and 213 showed a strong signal in all libraries, indicating that they represent genes expressed in multiple stages within the *D. iridis* lifecycle. Clone #50 displays a weak signal in amoebal, a weaker signal in zygote and a strong signal in plasmodial. This suggests a knockdown during the amoebae-zygote transition. This can also indicate the gene is important in plasmodial function. It is possible that this gene is expressed continuously but has an augmented use within plasmodia. Such myosin proteins could function in flagella motor proteins in amoebae and cytoplasmic streaming proteins in plasmodia.

Clone #145 shows a weak signal within amoebal library, a strong signal within the zygote library, and a weak signal in plasmodial suggesting that it may encode a gene involved in the amoebae-plasmodia transition. Clone #163 shows a strong signal in amoebael libraries, no signal in zygote and a weak signal in plasmodial; this suggests that this gene may be knocked down during the amoebae-plasmodia transition due to its absence in the zygote library. Likewise, clone #168 also shows a strong signal in amoebae, no signal in zygote, and a weak signal in plasmodia. The PCR products between plasmodial and amoebal libraries however are different sizes. This may suggest that clone #168 may belong to a gene with multiple isotypes between the two cell stages. Such distinction between isotypes is not uncommon in myxomycetes as many cytoskeletal proteins contain distinct amoebal, plasmodial, or sporulation isotypes (Bailey et al. 1995, Barrantes et al. 2012, T'Jampens et al. 1999). If the gene associated with clone #168 has conserved sequences between the amoebae and plasmodia isotypes then one could expect to see slightly different product sizes like we observe.

Clone #193 shows a strong signal in both amoebae and zygote libraries and a weak signal in plasmodia. This clone likely represents an amoebal gene that gets knocked down during or shortly after zygote development. Likewise, this clone contains an additional band within the plasmodia PCR products indicating it may also contain an isotype for both amoebae and plasmodia.

Limitations of our RT-PCR setup should be mentioned due to the ambiguity of our results. Since the zygote mRNA was not subtracted it contained genes from amoebae, zygote and plasmodial stages. Future experiments should include subtracted zygote cDNA libraries to obtain a more accurate depiction of zygote-specific genes.

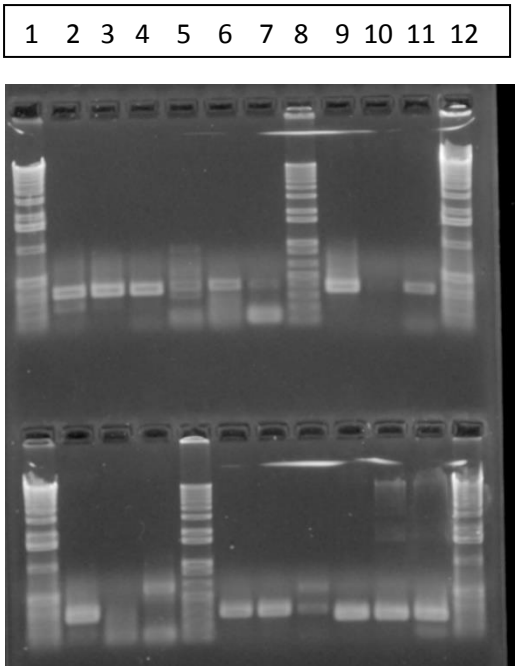

Lane (top)	Clone # (mRNA)	Lane (bot.)	Clone # (mRNA)
1	1 kb+	1	1 kb+
2	#14 (A)	2	#168 (A)
3	#14 (Z)	3	#168 (Z)
4	#14 (P)	4	#168 (P)
5	#145 (A)	5	1 kb+
6	#145 (Z)	6	#193 (A)
7	#145 (P)	7	#193 (Z)
8	1 kb+	8	#193 (P)
9	#163 (A)	9	#213 (A)
10	#163 (Z)	10	#213 (Z)
11	#163 (P)	11	#213 (P)
12	1 kb+	12	1 kb+

Figure 14. RT-PCR (1): Each lane represents a different mRNA population exposed to primers associated with a particular clone. Smears near the bottom of the lanes indicate primer dimers and are not indicative of a positive PCR product.

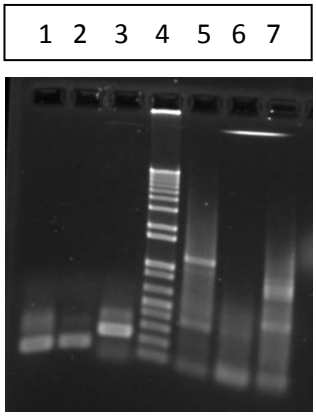

Lane	Clone # (mRNA)
1	#50 (A)
2	#50 (Z)
3	#50 (P)
4	1 kb+
5	#58 (A)
6	#58 (Z)
7	#58 (P)

Figure 15. RT-PCR (2): Each lane represents a different mRNA population exposed to primers associated with a particular clone. Smears near the bottom of the lanes indicate primer dimers and are not indicative of a positive PCR product.

Conclusion:

The zygote cell stage represents a pivotal and understudied time point in the myxomycete life cycle. It is within this stage that an irreversible developmental transition from haploid amoebae into diploid plasmodia occurs. Changes in cytoskeleton composition, cellular signaling, and protein translation are coupled with mitochondrial DNA degradation, and nuclear DNA proliferation; all occurring simultaneously in a relatively short time period. Understanding this developmental transition is critical to discovering novel myxomycete genes related to plasmodial development. We have identified genes involved in cytoskeletal composition and rearrangement, cell signaling, ubiquitin-proteasome pathway proteins, and other DNA binding proteins potentially involved in mitochondrial inheritance or transcription. We have also identified genes involved in metabolism, housekeeping and miscellaneous functions that can be seen in appendix C. These proteins may be useful in other myxomycete studies. Many follow up experiments can be conducted using data gathered from this study including biochemical protein analysis, gene expression assays, RT-PCR, and RNA interference studies.

Works Cited:

Alim, K., Andrew, N., Pringle, A., and Brenner, M.P. (2017). Mechanism of signal propagation in *Physarum polycephalum*. Proceedings of the National Academy of Sciences *114*, 5136-5141.

Altschul, S.F., Gish, W., Miller, W., Myers, E.W. & Lipman, D.J. (1990) "Basic local alignment search tool." J. Mol. Biol. 215:403-410

Bailey, J. (1995). Plasmodium development in the myxomycete *Physarum polycephalum*: genetic control and cellular events. Microbiology (Reading, England) *141 (Pt 10)*, 2355-2365.

Bailey, J., Anderson, R.W., and Dee, J. (1987). Growth and development in relation to the cell cycle in *Physarum polycephalum*. Protoplasma *141*, 101-111.

Bailey, J., Cook, L.J., Kilmer-Barber, R., Swanston, E., Solnica-Krezel, L., Lohman, K., Dove, W.F., Dee, J., and Anderson, R.W. (1999). Identification of three genes expressed primarily during development in *Physarum polycephalum*. Archives of microbiology *172*, 364-376.

Bailey, J., Solnica-Krezel, L., Lohman, K., Dee, J., Anderson, R.W., and Dove, W.F. (1992). Cellular and molecular analysis of plasmodium development in Physarum. Cell biology international reports *16*, 1083-1090.

Barr, C.M., Neiman, M., and Taylor, D.R. (2005). Inheritance and recombination of mitochondrial genomes in plants, fungi and animals. New Phytologist *168*, 39-50.

Barrantes, I., Leipzig, J., and Marwan, W. (2012). A next-generation sequencing approach to study the transcriptomic changes during the differentiation of Physarum at the single-cell level. Gene regulation and systems biology *6*, 127-137.

Boussard, A., Delescluse, J., Perez-Escudero, A., and Dussutour, A. (2019). Memory inception and preservation in slime moulds: the quest for a common mechanism. Philosophical transactions of the Royal Society of London Series B, Biological sciences *374*, 20180368.

Breton, S., and Stewart, D.T. (2015). Atypical mitochondrial inheritance patterns in eukaryotes. Genome *58*, 423-431.

Burland, T.G., Solnica-Krezel, L., Bailey, J., Cunningham, D.B., and Dove, W.F. (1993). Patterns of inheritance, development and the mitotic cycle in the protist *Physarum polycephalum*. Advances in microbial physiology *35*, 13-33.

Clark, J., Collins, O. R. & Tang, H.-C. *Didymium iridis* mating systems: partial compatibility between mating series. *Mycologia* 83, 210-213 (1991).

Clontech Laboratories, i. (2014). Plasmid DNA purification User manual NucleoSpin® Plasmid EasyPure.

Clontech Laboratories, i. (2014). SMARTer™ PCRcDNA Synthesis Kit User Manual. *Protocol No. PT4097-1*

Clontech Laboratories, i. (2016). Clontech® PCR-Select™ Bacterial Genome Subtraction KitUser Manual. *Protocal No. PT3170-1*.

Collins, O.R. (1976). Heterothallism and homothallism: a study of 27 isolates of *Didymium iridis*, a true slime mold. American Journal of Botany *63*, 138-143.

Collins, O.R., and Betterley, D.A. (1982). *Didymium iridis* in past and future research. In Cell Biology of Physarum and Didymium, J.W. Daniel, ed. (Academic Press), pp. 25-57.

de Lacy Costello, B., and Adamatzky, A.I. (2014). Routing of *Physarum polycephalum* "signals" using simple chemicals. Communicative & integrative biology *7*, e28543-e28543.

Diatchenko, L., Lau, Y.F., Campbell, A.P., Chenchik, A., Moqadam, F., Huang, B., Lukyanov, S., Lukyanov, K., Gurskaya, N., Sverdlov, E.D., *et al.* (1996). Suppression subtractive hybridization: a method for generating differentially regulated or tissue-specific cDNA probes and libraries. Proceedings of the National Academy of Sciences of the United States of America *93*, 6025-6030.

Eberhard, W.G. (1980). Evolutionary consequences of intracellular organelle competition. The Quarterly review of biology *55*, 231-249.

Fiore-Donno, A.M., Meyer, M., Baldauf, S.L., and Pawlowski, J. (2008). Evolution of dark-spored Myxomycetes (slime-molds): molecules versus morphology. Molecular phylogenetics and evolution *46*, 878-889.

Frederick, L. (1990). Phylum plasmodial slime molds class myxomycota. In Handbook of Protoctista: the Structure, Cultivation, Habitats and Life Histories of the Eukaryotic Microorganisms and their Descendents Exclusive of Animals, Plants and Fungi; a Guide to the Algae, Ciliates, Foraminifera, Sporozoa, Water Molds, Slime Molds and other Protoctists (Jones and Bartlett), pp. 467-483.

Glöckner, G., and Marwan, W. (2017). Transcriptome reprogramming during developmental switching in *Physarum polycephalum* involves extensive remodeling of intracellular signaling networks. Scientific Reports *7*, 12304.

Gray, M.W., Burger, G., and Lang, B.F. (1999). Mitochondrial evolution. Science *283*, 1476-1481.

Hadjivasiliou, Z., Lane, N., Seymour, R.M., and Pomiankowski, A. (2013). Dynamics of mitochondrial inheritance in the evolution of binary mating types and two sexes. Proceedings Biological Sciences *280*, 20131920.

Heidel, A.J., Lawal, H.M., Felder, M., Schilde, C., Helps, N.R., Tunggal, B., Rivero, F., John, U., Schleicher, M., Eichinger, L., *et al.* (2011). Phylogeny-wide analysis of social amoeba genomes highlights ancient origins for complex intercellular communication. Genome research *21*, 1882-1891.

Invitrogen (2013). One Shot® TOP10 Competent Cells. *Document Part Number 280126*.

Invitrogen (2016). SuperScript™ III One-Step RT-PCR System with Platinum™Taq DNAPolymerase. Doc. Part No. 12574.pps

Itoh, K., Izumi, A., Mori, T., Dohmae, N., Yui, R., Maeda-Sano, K., Shirai, Y., Kanaoka, M.M., Kuroiwa, T., Higashiyama, T., *et al.* (2011). DNA packaging proteins *Glom* and *Glom2* coordinately organize the mitochondrial nucleoid of *Physarum polycephalum*. Mitochondrion *11*, 575-586.

Kawano, S., Anderson, R.W., Nanba, T., and Kuroiwa, T. (1987). Polymorphism and uniparental inheritance of mitochondrial DNA in *Physarum polycephalum*. Journal of General Microbiology *133*, 3175-3182.

Laffler, T.G. (1987). Negative control of periodic tubulin gene expression in the mitotic cycle of *Physarum polycephalum*. European journal of cell biology *43*, 179-181.

Lekunberri, I., Subirats, J., Borrego, C.M., and Balcazar, J.L. (2017). Exploring the contribution of bacteriophages to antibiotic resistance. Environmental pollution (Barking, Essex : 1987) *220*, 981-984.

Moriyama, Y., Itoh, K., Nomura, H., and Kawano, S. (2009). Disappearance of mtDNA during mating of the true slime mold *Didymium iridis*. Cytologia *74*, 159-164.

Moriyama, Y., and Kawano, S. (2003). Rapid, selective digestion of mitochondrial DNA in accordance with the *matA* hierarchy of multiallelic mating types in the mitochondrial inheritance of *Physarum polycephalum*. Genetics *164*, 963-975.

Moriyama, Y., and Kawano, S. (2010). Maternal inheritance of mitochondria: multipolarity, multiallelism and hierarchical transmission of mitochondrial DNA in the true slime mold *Physarum polycephalum*. Journal of Plant Research *123*, 139-148.

Moriyama, Y., Yamazaki, T., Nomura, H., Sasaki, N., and Kawano, S. (2005). Early zygote-specific nuclease in mitochondria of the true slime mold *Physarum polycephalum*. Current genetics *48*, 334-343.

Morozov, A.V., and Karpov, V.L. (2018). Biological consequences of structural and functional proteasome diversity. Heliyon *4*, e00894.

Murray, M., Foxon, J., Sweeney, F., and Orr, E. (1994). Identification, partial sequence and genetic analysis of *mlpA*, a novel gene encoding a myosin-related protein in *Physarum polycephalum*. Current genetics *25*, 114-121.

Nandi, D., Tahiliani, P., Kumar, A., and Chandu, D. (2006). The ubiquitin-proteasome system. Journal of biosciences *31*, 137-155.

New England BioLabs. (2018). Magnetic mRNA Isolation Kit. *Protocal No. #S1550S*.

Pinchai, N., Lee, B.S., and Holler, E. (2006). Stage specific expression of poly(malic acid)-affiliated genes in the life cycle of *Physarum polycephalum*. Spherulin 3b and polymalatase. The FEBS journal *273*, 1046-1055.

Qiagen (2012). Oligotex® Handbook 104.

Roche (2004). DIG DNA Labeling and Detection Kit.

Ross, I.K. (1967). Syngamy and plasmodium formation in the Myxomycete *Didymium iridis*. Protoplasma *64*, 104-119.

Sato, M., and Sato, K. (2013). Maternal inheritance of mitochondrial DNA by diverse mechanisms to eliminate paternal mitochondrial DNA. Biochimica et biophysica acta *1833*, 1979-1984.

Schaap, P., Barrantes, I., Minx, P., Sasaki, N., Anderson, R.W., Benard, M., Biggar, K.K., Buchler, N.E., Bundschuh, R., Chen, X., *et al.* (2015). The *Physarum polycephalum* genome reveals extensive use of prokaryotic two-component and Metazoan-type tyrosine kinase signaling. Genome biology and evolution *8*, 109-125.

Scheer, M., and Silliker, M. (2006). Mitochondrial inheritance patterns in *Didymium iridis* are not influenced by stage of mating competency. Mycologia *98*, 51-56.

Sequencher® version 5.4.6 (2019) DNA sequence analysis software, Gene Codes Corporation, Ann Arbor, MI USA

Silliker, M.E., and Collins, O.R. (1988). Non-mendelian inheritance of mitochondrial DNA and ribosomal DNA in the myxomycete, *Didymium iridis*. Molecular Genetics and Genomics *213*, 370-378.

Silliker, M.E., Gong, T., and Collins, O.N.R. (1988). Spore-to-spore cultivation of *Didymium iridis* on heat-killed bacteria. Mycologia *80*, 151-156.

Silliker, M.E., Liles, J.L., and Monroe, J.A. (2002). Patterns of mitochondrial inheritance in the myxogastrid *Didymium iridis*. Mycologia *94*, 939-946.

Smith, G.E., and Summers, M.D. (1980). The bidirectional transfer of DNA and RNA to nitrocellulose or diazobenzyloxymethyl-paper. Analytical biochemistry *109*, 123-129.

Swiss Institute of Bioinformatics. (2019). ExPasy Bioinformatics Resource Portal. In Translate tool.

Solnica-Krezel, L., Bailey, J., Gruer, D.P., Price, J.M., Dove, W.F., Dee, J., and Anderson, R.W. (1995). Characterization of npf mutants identifying developmental genes in Physarum. Microbiology (Reading, England) *141 (Pt 4)*, 799-816.

Stephenson, S., and Stemphen, H. (2000). Myxomycetes: a handbook of slime molds (Timber Press).

Sweeney, G.E., Watts, D.I., and Turnock, G. (1987). Differential gene expression during the amoebal-plasmodial transition in Physarum. Nucleic acids research *15*, 933-945.

T'Jampens, D., Bailey, J., Cook, L.J., Constantin, B., Vandekerckhove, J., and Gettemans, J. (1999). Physarum amoebae express a distinct fragmin-like actin-binding protein that controls in vitro phosphorylation of actin by the actin-fragmin kinase. European journal of biochemistry *265*, 240-250.

T'Jampens, D., Meerschaert, K., Constantin, B., Bailey, J., Cook, L.J., De Corte, V., De Mol, H., Goethals, M., Van Damme, J., Vandekerckhove, J., *et al.* (1997). Molecular cloning, over-expression, developmental regulation and immunolocalization of fragminP, a gelsolin-related actin-binding protein from *Physarum polycephalum* plasmodia. Journal of cell science *110 (Pt 10)*, 1215-1226.

Turnock, G., Morris, S.R., and Dee, J. (1981). A comparison of the proteins of the amoebal and plasmodial phases of the slime mould, *Physarum polycephalum*. European journal of biochemistry *115*, 533-538.

UniProt (2019). UniProtKB - P03631 (REPA_BPPHS). In Replication associated protein A (Uniprot Consortium).

UniProt (2019). UniProtKB - P03639 (LYS_BPPHS). In Lysis Protein E (Uniprot Consortium).

UniProt (2019). UniProtKB - P69487 (SCAFD_BPS13). In External scaffolding protein D (Uniprot Consortium).

Uyeda, T.Q., and Kohama, K. (1987). Myosin switching during amoebo-plasmodial differentiation of slime mold, *Physarum polycephalum*. Experimental cell research *169*, 74-84.

Walker, L.M., Hoppe, T., and Silliker, M.E. (2017). Molecular techniques and current research approaches. In Myxomycetes, C. Rojas, ed. (Academic Press), pp. 145-173.

Walter, P., Hoffmann, X.K., Ebeling, B., Haas, M., and Marwan, W. (2013). Switch-like reprogramming of gene expression after fusion of multinucleate plasmodial cells of two *Physarum polycephalum* sporulation mutants. Biochemical and biophysical research communications *435*, 88-93.

Yu, Z., O'Farrell, P.H., Yakubovich, N., and DeLuca, S.Z. (2017). The mitochondrial DNA polymerase promotes elimination of paternal mitochondrial genomes. Current Biology *27*, 1033-1039.

Zientara-Rytter, K., and Subramani, S. (2019). The roles of ubiquitin-binding protein shuttles in the degradative fate of ubiquitinated proteins in the ubiquitin-proteasome system and autophagy. Cells *8*.

Appendix A:

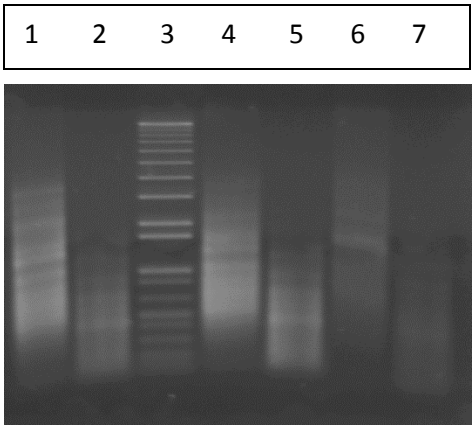

Lane	DNA
1	Tester pre RSA
2	Tester post RSA
3	1 kb marker
4	Driver pre RSA
5	Driver post RSA
6	Control pre RSA
7	Control post RSA

Figure 1. RSA digestion from zygote-amoebae subtraction sample: Following cDNA generation, our cDNA libraries were cut using the restriction enzyme RSA-I in order to obtain smaller DNA fragments. Successful digestion was indicated by smaller DNA fragments seen in the post RSA samples.

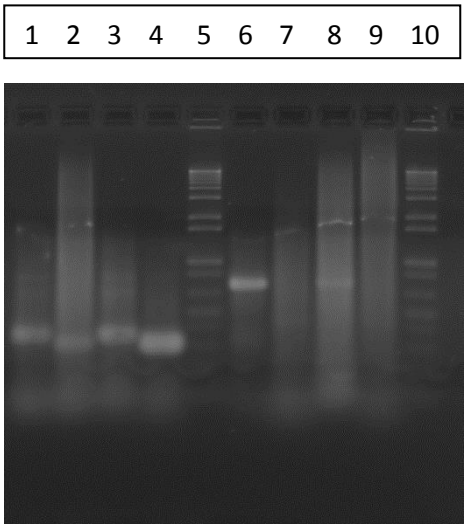

Lane	DNA	Primers
1	Driver	PCR 1, Pro A up
2	Driver	Pro A up/ down
3	Driver	PCR 1, Pro A up
4	Driver	Pro A up/ down
5	1kb marker	-
6	Control	PCR 1, G3PHD 3’
7	Control	G3PHD 3’, G3PHD 5’
8	Control	PCR 1, G3PHD 3’
9	Control	G3PHD 3’, G3PHD 5’
10	1kb marker	-

Figure 2. Ligation efficiency from zygote-amoebae subtraction sample: DNA was ligated with specific adapters for SSH and the efficiency of the ligation was analyzed using PCR followed by gel electrophoresis. Primers specific to the adapters were used in lanes 1, 3, 6 and 8 (PCR Primer 1) while primers located within transcripts were used in lanes 2, 4, 7 and 9. The profilin A gene was chosen based on previous data suggesting a high abundance in amoebae cell types. The G3PHD primers were provided with the kit and are flanking a gene known to be contained within transcripts in the control DNA. This image verifies a successful ligation of subtracted samples and an unsuccessful ligation of control samples.

Appendix B:

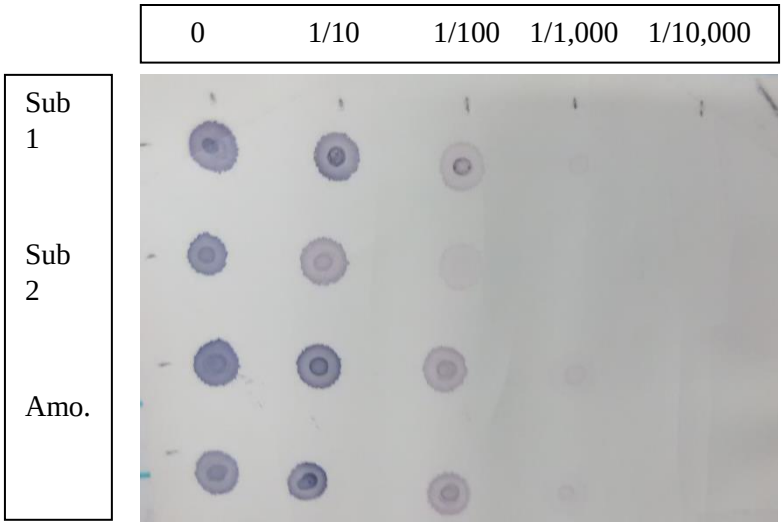

Figure 1. DIG labelling efficiency: Labeled probes were blotted onto a nylon membrane and tested for adequate incorporation of DIG-labelled nucleotides. Row are subtracted 1, subtracted 2, amoebae and plasmodia (top to bottom). Dilutions from left to right are (1:1, 1:10, 1:100, 1:1,000, 1:10,000).

Appendix C:

Table I: Complete list of annotated proteins

Clone # (ORF size)	Protein shared domain	Organism overlapped	E value	Possible function
5[i] (545 BP)	*	*	*	*
7 (283 BP)	Ribonuclease E (RNase E_G_superfamily)	*Saccoglossus kowalevskii* (acorn worm)	4e-05	Nuclease activity, cleaves ssRNA
10[ii] (272 BP)	P[i]rin domain (YhaK_superfamily)	*Acanthamoeba castellanii* (amoebae)	1e-56	DNA clustering, likely involved in transcription regulation
14 (646 BP)	*	*	*	*
15 (475 BP)	Dehydrogenase/ metabolic (NADB_Rossman superfamily)	*Cavenderia fasciculate* & *Dictyostelium discoideum* (cellular slime molds)	5e-110	Metabolism
17 (392 BP)	Elongation factor 1 (Selb_superfamily)	*Clastoderma debaryanum* (myxomycete)	1e-77	Ribosome synthesis
18/ 221[iii] (467/ 472 BP)	Strictosidine synthase family protein	Silene latifolia (flowering plant)	3e-3	Amine lyase that cleaves C-N bond and is used in alkaloid synthesis
19 (446 BP)	Initiation factor (DEXDc_superfamily)	*Arabidopsis thaliana* (angiosperm)	9e-84	Ribosome translation
20 (706 BP)	NAD(P)H Quinone oxoreductase (PIG3_family)	*Thamnocephalis sphaerospora* (fungus)	2e-45	Redox protein
21/ 162/ 178 (700 BP)	Hypothetical protein, DOC2	*Sphaeroforma arctica* (multi-nucleated protist), Piromyces (obligate anaerobe that lacks mt)	1e-29	"Extracellular serine rich", homolog is Ca^{2+} dependent and used in exocytosis
23/ 80 (461 /464 BP)	Myosin binding protein C	*Homo sapiens* (human)	1e-89	Heart muscle development
24/ 202 (422 / 608 BP)	Phosphoketolase (XFP_C_superfamily)	Amycolatopsis, (cyanobacteria)	1e-82, 2e-11	Metabolism, lyase
27 (348 BP)	Carboxylic ester hydrolase	*Cavenderia fasciculata* (cellular slime mold)	1e-18	Metabolic, often involved in detoxification of toxins
28/ 50 (504/ 519 BP)	*	*	*	*
33 (593 BP)	actin-binding protein fragmin P	*Physarum polycephalum*	2e-80	Cytoskeletal protein
63	Ubiquitin 4 (Ubq_superfamily)	*Physarum polycephalum*	6e-149	Proteostasis

(684 BP)				
65 (177 BP)	Pyruvate kinase	*Dictyostelium discoideum*	1e-19	Metabolism
73 (828 BP)	Beta actin (NBD_sugar_kinase_HSP70_actin family)	*Didymium squamulosum*	4e-154	Cytoskeleton, plasmodia development
76 (413 BP)	phosphoribosylformylglycinamidine synthase	*Coremiostelium polycephalum*	9e-61	Metabolism, purine biosynthesis
77 (541 BP)	Actin	*Physarum polycephalum*	6e-96	Cytoskeleton, plasmodia development
88 (528 BP)	Ubiquitin 4 (ubq superfamily)	*Physarum polycephalum*	8e-60	Ubiquitin proteasome pathway
97	hypothetical protein, SNF2-related domain-containing protein	*Cavenderia fasciculate* (cellular slime mold)	1e-9, 5e-6	Microtubule organization or mitotic process
104 (108 BP)	Oxidoreductase molybdopterin binding domain (SO_family_moco superfamily)	Acanthamoeba castellanii (amoebae)	4e-24	Redox reactions
111 (123 BP)	Glycine cleavage system protein R (ACT_superfamily)	Candidatus *Thiodiazotropha endoloripes* (bacteria)	3e-09	Breaks down glycine, located in mito
139 (121 BP)	Cytochrome p450	Pongo abelii (orangutan),	1e-08	Metabolism or drug detox
140 (184 BP)	Extracellular matrix protein B	*Tieghemostelium lacteum* (cellular slime mold)	2e-22	Extracellular matrix organization; used by cellular slime molds as a prestalk protein
143 (235 BP)	Xylulose-5-phosphate phosphoketolase	Candidatus *Rubidus massiliensis* (bacteria)	4e-25	Metabolism, lyase
144 (235 BP)	Ankyrin repeat and SOCS box containing-8	Homo sapien (human)	0.0 – 1e-180	Ubiquitination/ protein degradation
145 (447 BP)	*	*	*	*
147 (449 BP)	FHA domain containing protein	*Acanthamoeba castellanii* (amoebae)	3e-69	Involved in cell growth regulation in *mycobacteria* and *Arabidopsis*
148/ 209a$_{iv}$ (177/ 173 BP)	Lysis protein E, external scaffolding protein D	*Xanthomonas citri* (gram neg. bacteria), Numerous enterobactericiae phages	3e-31, 3e-29	Induce cell lysis by inhibiting lipid synthesis
148/ 209b (120/ 116 BP)	DNA Binding protein	*Salmonella enterica* (gram neg. bacteria)	1e-15, 6e-15	DNA binding domain
150 (336 BP)	LIM-type zinc finger-containing protein/ arrestin domain-containing protein	*Dictyostellium discoideum* (cellular slime mold)	3e-40	Signal transduction, vacuole organization
151/ 195 (257/ 344 BP)	SAM-dependent methyl transferase (AdoMet_MTases_superfamily)	*Acidobacteria bacterium* (gram neg. bacteria)	2e-39/ 4e-50	Methyl transfers/ ubiquitination probably
153 (254 BP)	Histidine kinase	Candidatus Fermentibacteria (gram pos. bacteria)	3e-32	Signal transduction

157 (669 BP)	*	*	*	*
159 (308 BP)	hexose phosphate transport system regulatory protein	*Planoprotostelium fungivorum* **(**Protosteliales**)**	7e-27	Transmembrane protein involved in signaling
160 (302 BP)	Clatherin heavy chain (Clathrin_superfamily)	*Acanthamoebae castellani* (amoebae)	7e-62	Vesicle coat
161 (455 BP)	DNA Topoisomerase II	*Physarym polycephalum*	3e-96	Cuts DNA strands (coiling)
163 (709 BP)	*	*	*	*
164 (354 BP)	26s proteasome regulatory sub unit 4 homolog A-like	*Chenopodium quinoa* (angiosperm)	3e-71	Degrades misfolded/ ubiquitinated proteins
165 (208 BP)	Phosphoketolase family protein	Streptomyces (gram pos. bacteria)	5e-25	Metabolism
166 (196 BP)	GPN-loop GTPase 2	*Cavenderia fasciculata* (cellular slime mold)	1e-18	GTPase activity
167 (150 BP)	EGF like domain	*Tieghemostelium lacteum* (cellular slime mold)	1e-09	Cell signaling, membrane receptor
168 (345 BP)	*	*	*	*
170/ 172 (425/ 425 BP)	*	*	*	*
171/ 189 (292/ 292 BP)	Tetrapeptide repeat homeobox 1	*Numida meleagris* (avian)	7e-06/ 7e-06	Encode DNA binding proteins/ development
173 (199 BP)	Structural maintenance of chromosome protein	*Tieghemostelium lacteum* (cellular slime mold)	2e-19	housekeeping
174 (248 BP)	Replication-associated protein A	*Escherichia coli* bacteriophage (viral)	3e-59	Viral DNA replication; properties prevent hydrolysis by nucleases and DNA rep. prevention
175 (715 BP)	Mitochondrial gene	*Plasmodiphora brassicae* (parasitic plant)	3e-05 (nucleotide seq)	Mt product, organism is multinucleated and infects plants
177/ 182 / 205/ 213/ 214/ 217/ 218/ 219 (403 BP)	*	*	*	*
180 (262 BP)	CAP-Gly containing linker protein 1	*Equus caballus* (horse)	4e-37 (0 for nucleotide)	Microtubule rearrangement
184 (436 BP)	RapGAP/RanGAP domain-containing protein	*Heterostelium album* (cellular slime mold)	5e-81	GTPase activity activator, possibly developmental
185 (518 BP)	1,4-alpha-glucan branching enzyme	*Dictyostellium discoideum* (cellular slime mold)	5e-117	Glycogen synthesis, metabolism
186/ 193 (734/ 773 BP)	*	*	*	*

187 (459 BP)	T-protein complex 1	*Calanus helgolandicus* (copepod)	1e-07 (nucleotide)	Involved in protein folding
188 (360 BP)	Hypothetical protein	*Acanthamoeba castellanii* (amoebae)	2e-46	Many hits to myxomycetes, possibly specific to the phylum
190 (235 BP)	Aldo-keto reductase	*Acanthamoeba castellanii* (amoebae)	1e-24	Metabolism, reduces aldehyde to alcohol, detoxification?
191 (186, 178 BP)	Hypothetical protein	*Stigmatella aurantiaca* (myxobacteria), burkholdia (pathogen)	8e-14, 5e-13	Both organisms seem to have high resistance to antibiotics
192/ 199 (736/ 761 BP)	*	*	*	*
194 (121 BP)	Hypothetical protein	*Planoprotostelium fungivorum* (Protosteliomycetes)	3e-04	
196 (554 BP)	NAD+ dependent glutamate dehydrogenase	*Cavenderia fasciculate* (cellular slime mold)	2e-111	Carbon/ nitrogen metabolism, urea production
197 (187 BP)	Ubiquitin-ligase like protein	*Tilletiopsis washingtonensis* (fungus)	3e-39	Involved in UBQ pathway, possible transfer or recruitment of UBQ ligase
200 (237 BP)	Anthranilate phosphoribosyltransferase	*Acanthamoeba castellanii* (amoebae)	1e-28	Amino acid synthesis by transfer of ribose on aromatic compounds
201 (78 BP)	phosphatidylinositide phosphatase SAC2-like	*Loxodonta africana* (elephant)	4e-04	Hydrolyzes phosphoric esters, metabolism
204 (204 BP)	*	*	*	*
207 (164 BP)	S-layer homology domain-containing protein	*Paenibacillus agaridevorans* (gram neg. bacteria)	1e-04	Associated with cell wall, possibly structure or signaling
208 (282 BP)	ras-related C3 botulinum toxin substrate 1-like	Acanthaster planci (starfish)	2e-60	G-protein activity, signal transduction and growth
210 (464 BP)	*	*	*	*
211 (389 BP)	Ras/GTPase domain containing protein	*Dictyostelium discoideum* (cellular slime mold)	1e-14	G-protein activity, signal transduction
211 (793 BP)	Troponin L1	*Homo sapiens* (human)	2e-132	Skeletal/ heart muscle protein
212/ 220 (392/ 392 BP)	*	*	*	*
213 (404 BP)	*	*	*	*
215/ 216a (337/ 337 BP)	Hypothetical protein	*Planoprotostelium fungivorum* (cellular slime mold)	3e-21	

215/ 216b (337/ 337 BP)	Armadillo-type protein, Elongation factor 3	*Lobosporangium transversal* (fungus), *Mortierella verticillata* (fungus)	9e-16, 7e-16	Interacts with DNA and usually binds to it or large proteins (ex. Helicases, ATPases) EF-3 is a protein involved in ribosome synthesis
301 (186 BP)	*	*	*	*
304 (476 BP)	Large ribosomal subunit	*Physarum polycephalum*	1e-92	Protein synthesis
305 (740 BP)	*	*	*	*
307 (155 BP)	cystathionine-beta-synthase domain-containing protein	*Cavenderia fasciculata* (cellular slime mold)	3e-06	Regulates enzymatic and protein domains
310 (187 BP)	uracil-DNA glycosylase	*Acanthamoeba castellanii* (amoebae)	2e-04	Removes Uracil's from DNA
312 (101 BP)	Hypothetical protein	*Acytostelium subglobosum* (cellular slime mold)	1e-09	-
313 (190 BP)	Hypothetical protein	*Planoprotostelium fungivorum* (cellular slime mold)	4e-03	
314 (250 BP)	Sry-box protein 9	*Eptatretus burger* (hagfish)	7e-12	Transcription factor that controls many development processes
315 (345 BP)	*	*	*	*
316 (287 BP)	*	*	*	*
317 (230 BP)	Adaptin earbinding coat-associated protein 2	*Acanthamoeba castellanii* (amoebae)	4e-35	Associated with transporting proteins or ions across the cell membrane
320/ 359 (343/ 343 BP)	*	*	*	*
321/ 325/ 360 (322/ 333/ 322 BP)	ADP-ribosylation factor (ras_superfamily)	*Heterostelium album* (cellular slime mold)	2e-55/ 1e-37/ 4e-54	GTP domain protein, involved in vesicle transport and actin remodeling
324 (126 BP)	tubulin polymerization-promoting protein family member 3	*Oryzias latipes* (fish)	4e-12	Cytoskeletal proteins; microtubule bundling/ formation
326/ 327 (311/ 306 BP)	pericentrin	*Homo sapiens* (human)	4e-95/ 2e-88	Mitotic spindle organization, possibly involved in cell cycle progression
328 (270 BP)	*	*	*	*

329 (142 BP)	Protein phosphatase 2C domain	*Acanthamoeba castellanii* (amoebae)	7e-07	Cell signaling/ kinase activity
330/ 343 (307/ 307 BP)	delta-12 fatty acid desaturase	Endogone sp. (fungus)	2e-54/ 5e-62	Involved in fatty acid synthesis
331 (710 BP)	kazel-type serine proteinase inhibitor	*Bombus terrestris* (bumble bee)	1e-05	Inhibits serine proteases and can act as toxin
332 (127 BP)	BTB/POZ domain containing protein	*Acanthamoeba castellanii* (amoebae)	3e-12	Likely acts as a substrate specific adapter to E3 ubiquitin ligase
333 (275 BP)	cystathionine-beta-synthase domain-containing protein	*Acanthamoeba castellanii* (amoebae)	8e-15	Regulates enzymatic activity
336 (346 BP)	Rab1 family GTPase	*Planoprotostelium fungivorum* (cellular slime mold)	8e-33	Monomeric G protein; signal transduction
338/ 354a (259 BP)	major histocompatibility complex II beta chain-like protein, partial	*Brugia malayi* (nematode)	1e-4	Immune cell recognition complex
338/ 354b (176 BP)	ribosomal protein L19	*Eimeria necatrix* (parasitic protist)	2e-9	Protein synthesis
340 (722 BP)	*	*	*	*
342 (211 BP)	Acetyl-CoA carboxylase	*Dictyostelium purpureum* (cellular slime mold)	5e-19	Fatty acid synthesis
345 (116 BP)	DNA Binding Protein	Pedobacter (gram neg. bacteria)	1e-15	DNA binding domain
346 (358 BP)	Pyruvate decarboxylase (TPP_enzyme_PYR superfamily)	Legionella spiritensis (gram neg bacteria)	2e-59	Enzyme that converts pyruvate into Acetyl-CoA
347 (605 BP)	cysteine desulfurase mitochondrial precursor (AAT_I superfamily)	*Planoprotostelium fungivorum* (protosteiales)	6e-90	Amino acid transferase, important in thiamine metabolism
353 (109 BP)	RHS repeat-associated core domain-containing protein	*Alloactinosynnema album* (cellular slime mold)	4e-10	Highly conserved, many involved in secreted toxins or intercellular signaling
356 (360 BP)	*	*	*	*
361 (743 BP)	*	*	*	*
363 (306 BP)	*	*	*	*
364 (237 BP)	*	*	*	*
366 (508 BP)	Cullin 3	*Dictyostellium discoideum* (cellular slime mold)	2e-92	Involved in ubiquitin protein ligase binding
368 (306 BP)	*	*	*	*
369 (113 BP)	FYN/Yes-like tyrosine-protein kinase	*Planoprotostelium fungivorum* (protosteiales)	1e-14	Intracellular signaling/ tyrosine kinase activity
370	*	*	*	*

(402 BP)				
371 (359 BP)	protein serine/threonine kinase (PKC_like_superfamily)	*Tieghemostelium lacteum* (cellular slime mold)	2e-84	Cell signaling which effects metabolism, proliferation, growth
372a (246 BP)	Synaptic vesicle 2-related protein (DIOX_N_superfamily)	*Symbiodinium microadriaticum* (dinoflagellate)	2e-41	Transmembrane transporter activity
372b (250 BP)	2-oxoglutarate (2OG) and Fe(II)-dependent oxygenase superfamily protein	*Klebsormidium nitens* (green algae)	4e-33	Citric acid cycle metabolism
376 (320 BP)	*	*	*	*
377 (285 BP)	HAT repeat-containing protein	*Heterostelium album* (cellular slime mold)	3e-06	Components of macromolecules involved in RNA processing; possibly protein-protein interactions
378/ 388 (221/ 206 BP)	Trehalosephosphatase (PLN02205_superfamily)	*Acanthamoeba castellanii* (amoebae)	4e-12 / 8e-13	Cleaves phosphate group from trehalose-6-phosphate; involved in increased desiccation resistance
379 (154 BP)	pre-mRNA-splicing factor cwc2	*Cavenderia fasciculate* (cellular slime mold)	2e-26	Involved in pre-mRNA splicing; needed for cell growth and cell cycle progression
386 (190 BP)	Rab GDP dissociation inhibitor alpha (NADB_Rossman_superfamily)	*Cavenderia fasciculata* (cellular slime mold)	2e-33	Regulates the GDP/GTP exchange of Rab proteins by inhibiting dissociation of GDP
387 (356 BP)	NADPH-cytochrome-P450 oxidoreductase	*Tieghemostelium lacteum* (cellular slime mold)	2e-75	Electron transfer from NADP to cytochrome p450; many downstream metabolic processes
390 (89 BP)	GCN20-type ATP-binding cassette protein GCN3, putative (SunT_superfamily)	*Entamoeba invadens* IP1 (Protazoan reptile parasite)	1e-04	Transmembrane transporter
391 (111 BP)	putative protein serine/threonine kinase (PKc_like_superfamily)	Cavenderia fasciculate (Cellular slime mold)	1e-12	Intracellular signaling kinase activity, possible cytoskeleton affiliation
392 (133 BP)	putative ribosomal protein L38 (Ribosomal_L38e_superfamily)	*Planoprotostelium fungivorum* (Protosteliales)	2e-14	Structural constituent of ribosome
394/ 401 (546 BP)	RGS-containing protein kinase RCK1	*Cavenderia fasciculate* (Cellular Slime Mold)	7e-12	Kinase Domain, Zinc Finger
398 (371 BP)	sugar-binding protein & RHS repeat-associated core domain-containing protein	*Alloactinosynnema album* (Gram positive bacteria)	8e-07	Intercellular signaling
399 (500 BP)	hypothetical protein	Dictyostelium discoideum (slime mold)	4e-16	Possibly specific to mycetazoa

[i]Clone number of clones that contained strong sequence data and open reading frames

[ii]Colors used to represent evolutionary lineages where green is mycetozoan and blue is amoebozoan

[iii]Clones containing overlapping transcripts were included in the same protein characterization and are shown using a /

[iv]Clones with denotations of "a" or "b" were used when two distinct proteins were identified to having comparably low e values